British Journal of Clinical Pharmacology

Br J Clin Pharmacol (2017) **83** 2426–2449 2426

PHARMACOKINETICS

ADAM, a hands-on patient simulator for teaching principles of drug disposition and compartmental pharmacokinetics

Correspondence Andrew Holt, Department of Pharmacology, 9-70 Medical Sciences Building, Faculty of Medicine and Dentistry, University of Alberta, Edmonton, Alberta, T6G 2H7, Canada. Tel.: +1 (780) 492 8620; Fax: +1 (780) 492 4325; E-mail: aholt@ualberta.ca

Received 1 February 2017; **Revised** 13 June 2017; **Accepted** 15 June 2017

Ines Zuna and Andrew Holt*

Department of Pharmacology, Faculty of Medicine and Dentistry, University of Alberta, Edmonton, Alberta, Canada

*Submitting author.

Keywords drug metabolism and pharmacokinetics, patient simulator, pharmacokinetics, teaching

AIMS

To design, construct and validate a pharmacokinetics simulator that offers students hands-on opportunities to participate in the design, administration and analysis of oral and intravenous dosing regimens.

METHODS

The Alberta Drug Administration Modeller (ADAM) is a mechanical patient in which peristaltic circulation of water through a network of silicone tubing and glass bottles creates a representation of the outcomes of drug absorption, distribution, metabolism and elimination. Changing peristaltic pump rates and volumes in bottles allows values for pharmacokinetic constants to be varied, thereby simulating differences in drug properties and in patient physiologies and pathologies. Following administration of methylene blue dye by oral or intravenous routes, plasma and/or urine samples are collected and drug concentrations are determined spectrophotometrically. The effectiveness of the simulator in enhancing student competence and confidence was assessed in two undergraduate laboratory classes.

RESULTS

The simulator effectively models one- and two-compartment drug behaviour in a mathematically-robust and realistic manner. Data allow calculation of numerous pharmacokinetic constants, by traditional graphing methods or with curve-fitting software. Students' competence in solving pharmacokinetic problems involving calculations and graphing improved significantly, while an increase in confidence and understanding was reported.

CONCLUSIONS

The ADAM is relatively inexpensive and straightforward to construct, and offers a realistic, hands-on pharmacokinetics learning opportunity for students that effectively complements didactic lectures.

DOI:10.1111/bcp.13357

WHAT IS ALREADY KNOWN ABOUT THIS SUBJECT

- Students struggle with pharmacokinetic concepts and calculations, in part because training in the subject offers few hands-on opportunities, particularly to preclinical students. This can subsequently result in dosing errors on the part of health professionals, and harm to patients.

WHAT THIS STUDY ADDS

- This study describes construction and use of a low-cost patient simulator that models compartmental pharmacokinetic behaviour in a mathematically-robust manner. Designed for use in an undergraduate laboratory, the simulator may also be adapted to demonstrate drug disposition in real time to a large audience in a lecture theatre.
- Data from summative assessment of student performance, as well as student feedback, indicated that the simulator was an effective teaching tool that could improve both competence and confidence beyond a level attained through an approach based only upon didactic lectures.

Introduction

Pharmacokinetics (PK) involves the application of mathematical principles and analyses to study the time-dependence of drug absorption, distribution, metabolism and elimination (ADME) [1, 2]. A working familiarity with the theory and practicalities of PK is important for a diverse clinical student population, including pharmacy, nursing and medical students [3], as well as for students of the life sciences – particularly pharmacology. Important competencies students are expected to acquire include determination of PK constants from quantitative biological sample data, designing drug dosing regimens based on these PK constants, correlating pharmacological responses with dosing parameters, understanding the effects of physiological and pathological conditions on drug disposition, and appropriately adjusting dosing parameters in disease states when necessary [1]. Although central to therapeutics, the subject of PK remains one of the most challenging to teach, and many students have considerable difficulty applying PK in different contexts [4, 5].

Traditionally, instructors present students in didactic lectures with mathematical and physiological principles underpinning PK, as well as applied examples [2, 5]. Somewhat unrealistically, students are often then expected to be able to handle data confidently, whether in examinations or in a patient setting [5]. Mastering problem-solving skills in clinical PK has been facilitated through small group discussions and tutorials [4]. Some instructors have expanded this approach by creating courses focused on team-based learning, case-based exercises [6], problem-based learning and even educational PK games [5, 7–9], while more interactive clinically-focused learning techniques involve computer simulations [4, 10], smartphone apps and online self-assessment tools [3, 11, 12]. Yet another approach highlights anecdotal experiences of clinical catastrophes in the teaching of medical students, with the authors noting that, typically, students are not adequately trained in PK for effective clinical translation [13].

A common thread running through most of these teaching strategies is a lack of realistic hands-on opportunities for those students, particularly in preclinical subjects, who do not have ready access to patient samples, limiting the scope for providing a clinical-like context to student learning. Historically, such opportunities may have involved the use of animals or human volunteers, but progressing ethical standards have rendered these practices largely obsolete. Here, we describe the development and testing of the Alberta Drug Administration Modeller (ADAM), a mechanical patient in which peristaltic circulation of water through a network of silicone tubing and glass bottles creates a mathematically-robust representation of the outcomes of drug ADME. A rudimentary system mimicking some of these outcomes had been described previously [14]; design of a more extensive modeller was inspired by a report, in *Pharmacology Matters*, of a novel teaching apparatus in which methylene blue dye was transferred between beakers by two peristaltic pumps to mimic clearance [15]. We adapted and expanded this idea to create a teaching tool that models all major aspects of PK behaviour, with quantitation of methylene blue in fluid samples that represent plasma or urine achieved through spectrophotometry. Inclusion in an undergraduate pharmacology laboratory course of two practical classes involving the modeller led to significant improvements in student understanding and enhanced student perceptions of their capabilities in handling PK data.

The purpose of this manuscript is thus to offer the reader some insight into the educational effectiveness of the apparatus, and to provide sufficient description to allow construction and operation of the apparatus as shown, or of a modified version suited to the varied teaching requirements of other institutions.

Methods

Apparatus concept and construction

The apparatus is composed primarily of six peristaltic pumps connected with Tygon tubing, through which water, representing the plasma, is circulated (Figure 1). The HEART pump (D) circulates the water within the main circuit (systemic circulation). Hepatic and renal clearance are controlled by the LIVER pump (G) and KIDNEY 1 pump (J), respectively. These pumps drain water (containing methylene blue) from the main circuit into hepatic waste (P), equivalent to drug and/or metabolites in faeces plus metabolites in urine, or into a urine beaker (O), equivalent to unchanged drug eliminated in urine. To maintain urine flow at a relatively constant rate, the volume of fluid pumped from the circulation into the urine beaker per minute by the KIDNEY 1 pump is supplemented with water supplied through the KIDNEY 2 pump (I), such that the combined outputs from both pumps is held

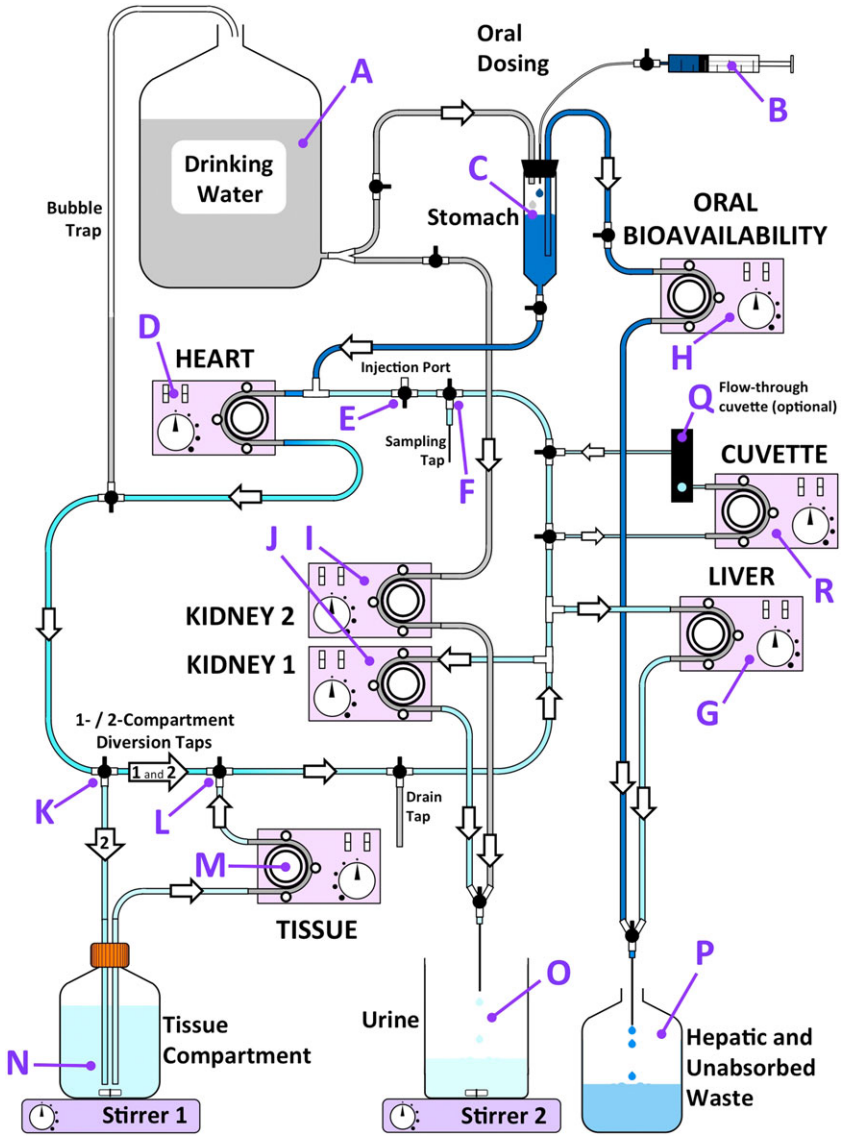

Figure 1

Schematic of the Alberta Drug Administration Modeller

constant, at around 8 ml min^{-1}. This allows renal clearance to be increased or decreased without changing the rate of urine production. The ORAL BIOAVAILABILITY pump (H) moves water containing orally-administered drug from the stomach (C), an airtight 50 ml conical tube, into hepatic waste in order to mimic incomplete absorption and/or first-pass metabolism.

The fluid volume lost from the circulation through the combined action of pumps G, H and J is replaced by drinking water (A), which is drawn into the air-tight stomach in response to fluid draining from the stomach.

An air-tight tissue compartment bottle (N) can be introduced by opening two diversion taps (K and L), allowing drug to be circulated both through the main circuit and, in parallel, through the tissue compartment, under the control of the TISSUE pump (M). Varying the volume of the tissue compartment bottle, or varying the speed of the TISSUE pump, alters the rate and extent of drug distribution.

Immediately upstream of the intravenous (IV) injection port, 3-way taps allow a portion of the flow to be redirected through a glass flow-through cuvette (Q) before returning to the systemic circulation, via another medium-flow peristaltic CUVETTE pump (R). Drug concentration can thus be monitored in real time by continuous monitoring of absorbance, without the need for collection of blood samples. The absorbance at 664 nm of fluid passing through the flow-through cuvette at 7 ml min^{-1} was measured in a Cary 60 spectrophotometer; this instrument may be operated with the sample chamber lid open, facilitating use of the flow-through cuvette.

Drug administration

Drug can be administered into the system orally, from a syringe (B) into an airtight 50 ml conical centrifuge tube representing the stomach (C). When drug was

administered by this route, a further 2 ml of water were injected to flush the entire dose of methylene blue from the cannula into the stomach. By changing the volume of liquid initially present in the stomach vessel, it is possible to change the absorption rate constant (k_{abs}) for the drug, as well as both the peak concentration of drug in plasma (C_{max}) and the time required to reach C_{max} (t_{max}). The degree to which these parameters can be modified can be expanded by increasing the volume of the stomach vessel. Adjusting the ORAL BIOAVAILABILITY pump (H) varies the proportion of the initial dose of drug that reaches the systemic circulation. Drug then passes from the stomach into the circulation as fluid moves from the stomach to replace that lost to hepatic and renal waste.

Drug can also be administered intravenously from a syringe via an injection port (E) comprised of a three-way tap with a luer fitting. On entering the systemic circulation, an intravenous bolus dose of drug typically completes around five circuits of the plasma compartment before mixing of drug with water representing blood is complete. As soon as drug is present in the main circuit, it can undergo elimination via the LIVER and KIDNEY 1 pumps, with kinetics that model elimination from a one-compartment system. However, by opening up the diversion taps (K and L) to include the TISSUE pump (M) and tissue compartment (N), it is possible to mimic two-compartment distribution and elimination behaviour.

At selected time points, samples (< 1 ml) are collected into microfuge tubes via the sampling port (F), or by collecting urine samples (O). Absorbance values for these samples are measured in a spectrophotometer or microplate reader at 664 nm and are then converted to concentrations (molar absorption coefficient 70 130 M^{-1} cm^{-1}). Concentration data are plotted *vs.* time on linear or semilogarithmic plots and data are fitted with appropriate equations to determine a variety of PK constants (See Table 1). When urine samples are collected, the cumulative urine volume is also measured at each time point so that the cumulative amount of drug eliminated in the urine may be determined; data are corrected to account for the urine removed for absorbance measurements.

The authenticity of data generated by the modeller was also assessed through use of a no-cost add-in program for Microsoft Excel, PKSolver [16]; this analytical tool is similar to Phoenix WinNonlin, a PK modelling software package used by many pharmaceutical companies.

In the classroom

The modeller was introduced into a 3rd-year experimental course for undergraduate pharmacology students at the University of Alberta, in two consecutive practical classes. Although graduating with a BSc degree, many of these students then go on to complete a professional degree in medicine or pharmacy at the University of Alberta, with further exposure to PK being particularly limited in the medical curriculum. It is thus important that the PK component of the pharmacology undergraduate program provides students with a thorough grasp of core concepts and an ability to translate these concepts to clinical situations.

During the classes, students worked in one of five small groups on a dedicated apparatus to obtain PK constants in their patient, and then to use these values to design a chronic dosing regimen. During the initial class, students administered a single dose of methylene blue to their patient by the IV and *per os* (PO) routes and collected blood and urine samples at suitable intervals prior to analysing concentration–time profiles. Prior to the second class, students were asked to design two chronic dosing regimens (an IV infusion regimen and a repeated oral dosing regimen in which peak and trough concentrations were required not to exceed the upper

Table 1

Pharmacokinetic equations used for experimental analyses reported in Tables 2–9

(1) $V_D = \frac{\text{Dose}}{C_{t0}}$	**(7)** $t_{\frac{1}{2}} = \frac{0.693}{k}$	**(13)** $\frac{C_{max}\text{ at steady state}}{C_{min}\text{ at steady state}} = \frac{1}{e^{-k_{el}\cdot\tau}}$
(2) $CL_{Total} = \frac{\text{Dose}\ (\times F)}{AUC_{t_{n-1}}^{t_n}}$	**(8)** $CL_R = \left(\frac{\text{Plateau}}{\text{Dose}}\right) \times CL_{Total}$	**(14)** $k_{12} = \frac{AB(\beta-\alpha)^2}{(A+B)(A\beta+B\alpha)}$
(3) $AUC_{t_{n-1}}^{t_n} = \frac{C_{t0}}{k_{el}}$	**(9)** $V_{D\ SS} = \frac{\left(\text{Dose} \times \left(\frac{A}{\alpha^2} + \frac{B}{\beta^2}\right)\right)}{AUC^2}$	**(15)** $k_{21} = \frac{(A\beta+B\alpha)}{A+B}$
(4) $AUC = \sum AUC_{t_{n-1}}^{t_n} + \frac{C_{tn}}{k_{el}}$	**(10)** $V_{D\ Area} = \frac{\text{Dose}}{(AUC \times \beta)}$	**(16)** $k_{10} = \frac{\alpha\beta(A+B)}{(A\beta+B\alpha)}$
(5) $F = \frac{AUC_{PO}}{AUC_{IV}}$	**(11)** $V_{D\ Extrap} = \frac{\text{Dose}}{B}$	**(17)** Oral Dose Rate $= \frac{\text{IV Dose Rate}}{F}$
(6) $-k$ = Slope × 2.303	**(12)** $C_{SS} = \frac{\text{Maintenance Dose Rate}}{V_D \times k_{el}}$	**(18)** Loading Dose = $C_{SS} \times V_D$

AUC, area under a concentration-time curve (time zero to infinity); α, first-order rate constant for distribution; β, first-order rate constant for elimination; CL, clearance; CL_R, renal clearance; CL_{Total}, total body clearance; C_{max}, peak plasma concentration after a single (PO) drug dose or mean peak plasma concentration with repeated dosing at steady state; C_{min}, mean trough plasma concentration with repeated dosing at steady state; C_{SS}, mean plasma concentration with repeated dosing at steady state; C_{t0}, concentration of drug in the plasma at t = 0; C_{tn}, concentration of drug in the plasma at t = n; F, oral bioavailability; k, first order rate constant; k_{10}, first order rate constant for elimination of drug from the central compartment only; k_{12}, first order rate constant for movement of drug from the central to the peripheral compartment; k_{21}, first order rate constant for movement of drug from the peripheral to the central compartment; k_{el}, first order rate constant for elimination; τ, dosing interval in a repeated dosing regimen; V_D, volume of distribution; $V_{D\ Area}$, volume of distribution calculated by the area or beta method; $V_{D\ SS}$, volume of distribution calculated by the steady state method; $V_{D\ Extrap}$, volume of distribution calculated from the Y-intercept of the terminal elimination phase

and lower limits of a therapeutic window) based upon PK parameters calculated from data obtained in the initial class. Patients were then subjected to both chronic regimens; once again, students sampled blood and generated plasma concentration–time profiles to confirm that PK targets had been achieved.

Plasma concentration–time profiles presented herein were obtained during development and assessment of the apparatus, rather than by students during a laboratory practical class.

The students, who had previously been exposed to principles of PK for 10 h in a 2nd-year lecture-based course, were also divided into two similar groups based upon examination performance for the purposes of assessing their ability to answer PK questions involving calculations or comprehension of core concepts. Before the first practical class, students completed a seven-question multiple choice test, with each group issued one of two different test versions. Questions provided students with descriptive text, or with numerical or graphical data, either in the form of PK constants for a given drug or of patient data, and required them to interpret or analyse the information, through application of concepts and/or use of appropriate equations, to determine further drug-specific parameters related to dosing, clearance, half-life or volume of distribution. Students were permitted unlimited time to complete the test. Following the second practical class, students completed the version of the test that they had not previously answered. Students were also asked to complete a self-assessment of their confidence and competence working with PK concepts and calculations. Consent was obtained retroactively to use results from tests and self-assessments, as approved by the Human Ethics Research Board at the University of Alberta (Study ID Pro00056323).

Materials

All Variable Flow Mini-Pump peristaltic pumps (Control Company, Friendswood, TX, USA) were purchased from VWR (Mississauga, Ontario, Canada) and were supplied with several different diameters of tubing that could be inserted between the rollers on the pump head to allow a wide range of flow rates. All pumps were calibrated gravimetrically across appropriate flow rate ranges.

Drinking water drained into the circulatory system via the stomach from a 5000 ml Kimax Reservoir bottle (VWR). The tissue compartment was comprised of a 250 ml or 1000 ml storage/media bottle (VWR) with a screw cap equipped with two hose connectors and air-tight gasket, manufactured by Duran Group (Mainz, Germany) and purchased as a special order item from Fisher Scientific (Ottawa, Ontario, Canada). The stomach was manufactured from a 50 ml conical centrifuge tube (Eppendorf; Mississauga, Ontario, Canada), with a hole drilled through the base of the tube and a luer-to-tubing barb fitting inserted and cemented in place. The tube was sealed with a rubber stopper drilled to accommodate three stainless tubes [2.38 mm outer diameter (od)], onto which short lengths of Tygon tubing [1/16″ (1.59 mm) inner diameter (id)] were attached to accommodate insertion of luer fittings or cannulae.

The circulatory system was comprised of Tygon tubing (1/4″ (6.35 mm) id, 3/8″ (9.52 mm) od), with a total volume for the main circuit of approximately 100 ml. Tubing was attached to other components of the apparatus through a variety of nylon luer fittings (Cole-Parmer, Montréal, Québec, Canada): one- and three-way stopcocks, T- and Y-connectors 1/4″ (6.35 mm), female luer fittings 1/4″ (6.35 mm), male luer lock rings 1/4″ (6.35 mm), wide-bore luer adapters: male luer lock to 1/16″ (1.59 mm) id, male luer plugs and several items from a luer fittings kit. Polyethylene tubing (1.19 mm id, 1.7 mm od; Becton Dickinson, Mississauga, Ontario, Canada) served to facilitate introduction of drug to the stomach from a syringe, to drain fluid from the system into hepatic or renal waste, to redirect a portion of the circulation via a flow-through cuvette, or as a conduit from the sampling tap.

Methylene blue was purchased from Sigma–Aldrich (Oakville, Ontario, Canada). Absorbance values of samples (300 µl) were read in polystyrene microplates (Greiner Bio-One; VWR), in a FlexStation 3 (Molecular Devices, Sunnyvale, CA, USA) with PathCheck activated. In some experiments, drug concentration was monitored continuously in a glass flow-through cuvette, in a Cary 60 UV–Visible spectrophotometer (Agilent Technologies, Mississauga, Ontario, Canada).

Results

One-compartment modelling

Circulating fluid through the main circuit with diversion taps closed to isolate the tissue compartment facilitates modelling of simple one-compartment kinetic behaviour that is evident when distribution is either extremely rapid, or negligible [17]. Figure 2 shows results from experiments in which identical drug doses were administered intravenously (IV) or *per os* (PO), all pump settings (with the exception of the ORAL BIOAVAILABILITY pump, which was turned on for the PO experiment but not for the IV experiment) being identical in both cases (Table 2). Area under the concentration-time curve (AUC) values for each data set were calculated as outlined in Table 2, with oral bioavailability determined as 29%. The ORAL BIOAVAILABILITY pump had been set at a rate 2.3× higher than the combined rates of LIVER and KIDNEY 1 pumps such that approximately 70% of drug in the stomach was transferred to waste without ever reaching the systemic circulation. The observed oral bioavailability was thus entirely consistent with the pump settings.

The tubing representing the systemic circulation has a capacity of approximately 100 ml; the volume of distribution (V_D), calculated from IV data was ~90 ml. A compound confined to the plasma will have a V_D value approximating the volume of the central compartment that will not change significantly with time [17], and this relationship is observed to hold true in ADAM.

Plotting those data points from Figure 2A that correspond solely to elimination on semilogarithmic axes yields straight lines (Figure 2B). Determination of slopes revealed elimination $t_{½}$ values of 9.4 and 9.9 min following IV and PO administration, respectively. This reflects consistent settings on KIDNEY 1 and LIVER pumps between the respective experiments.

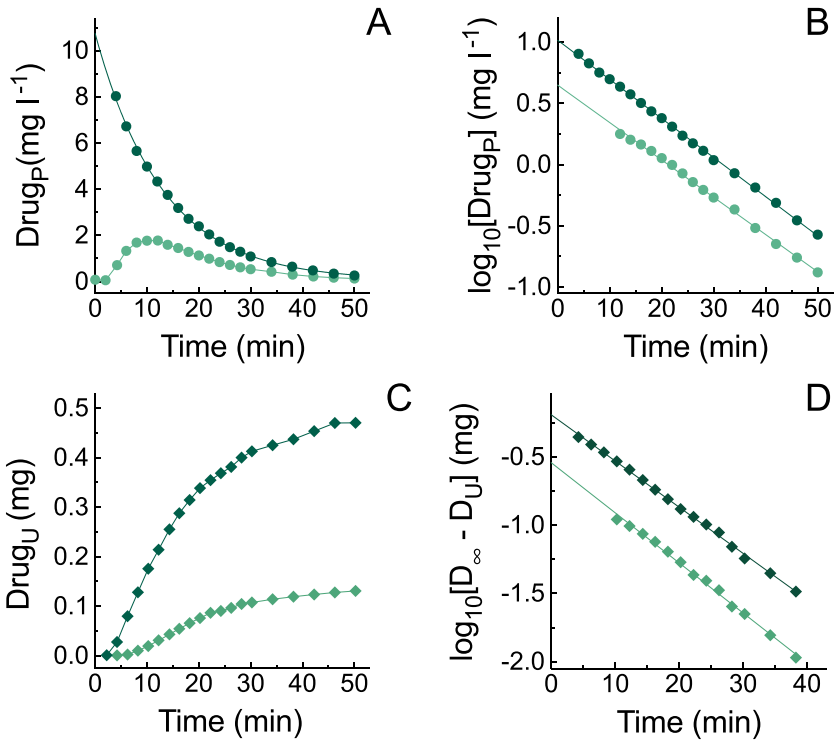

Figure 2

One-compartment modelling of plasma and urinary drug concentrations following intravenous (IV) and *per os* (PO) administration. Calculated pharmacokinetics (PK) parameters are shown in Table 2. (A) Drug in plasma following IV (●) and PO (●) administration. (B) Classical semilogarithmic plots of IV (●) and PO (●) elimination data from (A) reveal similar slopes. (C) Cumulative drug in urine following IV (◆) and PO (◆) administration. (D) Analysis of IV (◆) and PO (◆) urinary data by the sigma-minus method reveals rate constants for renal elimination similar to those obtained from plasma. Pump settings were: HEART pump: 132 ml min^{-1}, LIVER pump: 3 ml min^{-1}, KIDNEY 1 pump: 3 ml min^{-1}, KIDNEY 2 pump: 4 ml min^{-1}, ORAL BIOAVAILABILITY PUMP: 24 ml min^{-1}

Several other parameters can be obtained from PO data; these are discussed in results from two-compartment experiments, below.

Plotting urinary data (Figure 2C) allowed estimation of plateau values corresponding to D_∞, which were used to calculate CL_R (Table 2). D_∞ values were then used to generate data shown in Figure 2D, the slopes from which allowed calculation of elimination $t_{½}$ values of 8.9 and 8.2 min following IV and PO administration, respectively.

Figures 3A and B show linear and semilogarithmic plots, respectively, of data obtained following IV administration of a single dose of drug, with combined hepatic and renal clearance set to either a high or a low rate. Table 3 confirms that parameters such as C_{t0} and V_D remained constant and were independent of clearance rates, while parameters associated with elimination, as well as AUC, reflected the altered pump settings. Figures 3C and D show linear and semilogarithmic plots, respectively, of data obtained following IV administration of a low and a high drug dose, with all pump settings consistent between experiments. Table 3 confirms that parameters associated with elimination remained constant, while differences in C_{t0} and AUC reflected the size of the doses administered. Further, as expected, the magnitude of V_D was constant, regardless of differences in total body clearance (Figures 3A and B) or in the doses administered (Figures 3C and D). These observations are consistent with one-compartment kinetic behaviour.

Repeated IV doses of drug were administered in the one-compartment model. Based on parameters calculated following a single IV administration (Figure 4 and Table 4), chronic dosing parameters were calculated that would achieve a steady state of 6 mg l^{-1} while maintaining a peak:trough ratio of 2, between 8 mg l^{-1} and 4 mg l^{-1} (Table 4). Results shown in Figure 4B confirm that the desired steady-state concentration (C_{SS}) was achieved, after approximately 5 half-lives of administration, with peak and trough concentrations remaining within the therapeutic window.

Two-compartment modelling

Figure 5A shows plots of example data obtained following a single IV dose of drug administered with the apparatus configured to model two-compartment kinetic behaviour. The semilogarithmic plot clearly illustrates the classical two-compartment *hockey-stick* curve. Following extrapolation of the terminal linear phase of this curve to the Y-axis, curve-stripping was done manually by the method of residuals to isolate and quantify the contribution of the distribution process to drug disappearance from the central compartment. Semilogarithmic plots of the separated distribution and elimination phases are shown in Figure 5B.

Table 2

Pharmacokinetic (PK) constants obtained from analyses of plasma and urinary drug concentrations following intravenous (IV) and *per os* (PO) administration, with the simulator in a one-compartment configuration (see Figure 2)

Figure 2A			
LIVER pump setting **KIDNEY 1 pump setting** **KIDNEY 2 pump setting** **Drug dose:** 0.96 mg		**3 ml min^{-1}** **3 ml min^{-1}** **4 ml min^{-1}** **Acute IV Administration**	
PK parameter	**Equation/method used**	**IV**	**PK Solver**
C_{t0}	Single-phase exponential decay fit	10.7 mg l^{-1}	9.6 mg l^{-1}
k	Single-phase exponential decay fit	0.077 min^{-1}	0.068 min^{-1}
$t_{1/2}$	Single-phase exponential decay fit	9.0 min	10.2 min
AUC_{IV}	Equation (3); Table 1; AUC = C_{t0} / k	139 min × mg l^{-1}	140 min × mg l^{-1}
V_D	Equation (1); Table 1; V_D = Dose / C_{t0}	89.9 ml	100 ml
CL_{Total}	Equation (2); Table 1; CL_{Total} = Dose / AUC	6.9 ml min^{-1}	6.8 ml min^{-1}
r^2	Single-phase exponential decay fit	0.9994	0.9936
ORAL BIOAVAILABILITY pump setting		**14 ml min^{-1}**	
Drug Dose: 0.96 mg		**Acute Oral Administration**	
PK parameter	**Equation/method used**	**PO**	**PK solver**
AUC_{PO}	Equation (4); Table 1; AUC = $\sum AUC_{t_{n-1}}^{t_n} + C_{tn}/k$	40.1 min × mg l^{-1}	40.3 min × mg l^{-1}
F	Equation (5); Table 1; F = (AUC_{PO} / AUC_{IV}) × 100	29.0%	28.8%
CL_{Total}	Equation (2); Table 1; CL_{Total} = (Dose × F) / AUC	6.9 ml min^{-1}	6.5 ml min^{-1}
Figure 2B			
PK parameter	**Equation/method used**	**IV**	**PO**
Y-intercept	Linear regression fit	1.015	0.649
C_{t0}	$10^{Y\text{–intercept}}$	10.35 mg l^{-1}	4.45 mg l^{-1}
slope	Linear regression fit	–0.032	–0.031
k	Equation (6); Table 1; –k = slope × 2.303	0.074 min^{-1}	0.070 min^{-1}
$t_{1/2}$	Equation (7); Table 1; $t_{1/2}$ = 0.693 / k	9.4 min	9.9 min
r^2	Linear regression fit	0.9995	0.9983
Figures 2C & 2D			
PK parameter	**Equation/method used**	**IV**	**PO**
plateau (D_∞)	Average of last three data points	0.465 mg	0.128 mg
slope	(D_∞-D_U) Nonlinear regression fit	–0.034	–0.037
k	Equation (6); Table 1; –k = slope × 2.303	0.078 min^{-1}	0.084 min^{-1}
$t_{1/2}$	Equation (7); Table 1; $t_{1/2}$ = 0.693 / k	8.9 min	8.2 min
CL_R	Equation (8); Table 1; CL_R = (Plateau / Total Dose) × CL_{Total}	3.4 ml min^{-1}	3.0 ml min^{-1}
r^2	(D_∞-D_U) Nonlinear regression fit	0.9985	0.9958

D_∞, amount of drug excreted in the urine at time = ∞; IV, intravenous (administration); $t_{1/2}$, half life

Table 5 lists pharmacokinetic parameters obtained through manual curve-stripping, as well as from fitting of a two-phase exponential equation to linear data, and reveals a high degree of consistency between values for parameters obtained by the two approaches. Parameters calculated with PKSolver software are also shown, and these too were consistent with those obtained through the other approaches.

The B-intercept value obtained by curve-stripping was used to calculate a volume of distribution of 453 ml (V_D

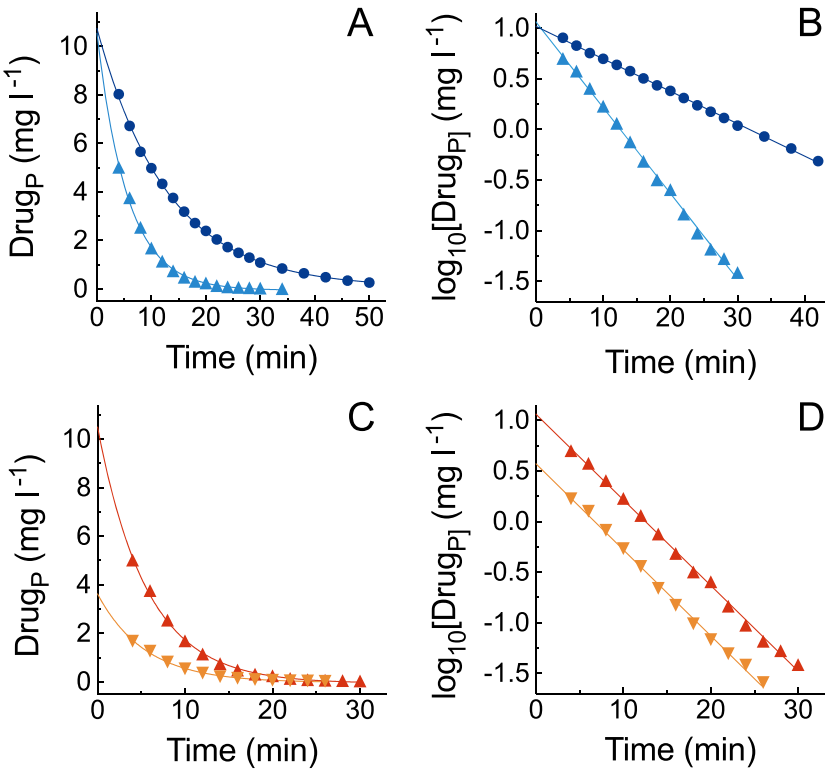

Figure 3

Effects of varying total body clearance or drug dose on plasma concentration–time profiles following intravenous (IV) administration in a one-compartment configuration. Calculated pharmacokinetic parameters are shown in Table 3. (A) Data were obtained following similar IV bolus doses, with *slow* (LIVER pump: 3 ml min^{-1}, KIDNEY 1 pump: 3 ml min^{-1}, KIDNEY 2 pump: 4 ml min^{-1}; ●) and *fast* (LIVER pump: 12 ml min^{-1}, KIDNEY 1 pump: 4 ml min^{-1}, KIDNEY 2 pump: 3 ml min^{-1}; ▲) elimination pump settings. (B) Semilogarithmic plots of data from (A). (C) Data were obtained following IV bolus doses of 0.96 mg (▲) and 0.32 mg (▼) methylene blue, with elimination pump settings identical to the *fast* settings used in (A), above. (D) Semilogarithmic plots of data from (C). In all experiments, the HEART pump setting was 132 ml min^{-1}

$_{Extrap}$; Table 5). This value is significantly higher than the sum of the central and peripheral compartment volumes of the apparatus. Although the extrapolation method to obtain a value for V_D is that most often taught to undergraduates, presumably because the approach follows on intuitively from that used to obtain V_D in a one-compartment model, $V_{D\ Extrap}$ is recognized as representing an over-estimation of volume [18]. Better estimates may be obtained from calculations of $V_{D\ Area}$ or $V_{D\ SS}$ [19]; the latter should provide the best estimate of the actual volume of water present in the modeller, and this was seen to be the case (Table 5).

The total body CL value calculated from Dose/AUC was determined to be 12.8 ml min^{-1}, reasonably consistent with the sum of the settings of the LIVER (7 ml min^{-1}) and KIDNEY 1 (3 ml min^{-1}) pumps (Table 5).

Curve-stripping allowed calculation of the distribution rate constant, α, as 0.45 min^{-1}, while the elimination rate constant, β, was calculated as 0.034 min^{-1}. In combination with the A-intercept extrapolated from the distribution phase (5.75 mg l^{-1}), and the B-intercept extrapolated from the elimination phase (2.12 mg l^{-1}; Figure 5B), these values allowed calculation of microconstants k_{12} and k_{21}, associated with drug transfer from the circulation to the tissue and from the tissue to the circulation, respectively [1], and k_{10}, associated with drug transfer exclusively from the central compartment to waste (Table 5). Of note, the calculated value for k_{10}, the microconstant for elimination of drug from the central compartment (of approximate volume 100 ml), was 0.10 min^{-1}; this correlates well with the sum of LIVER and KIDNEY 1 pump rates in this experiment, which was 10 ml min^{-1}. Equivalent one-compartment k values of 0.077 min^{-1} and 0.179 min^{-1} were obtained when combined clearance pump rates were 6 and 18 ml min^{-1}, respectively (Figure 3), also consistent with the value determined here for k_{10}.

Figure 5C shows cumulative urinary data from the same experiment, from which an estimate was obtained for the total amount of drug eliminated in the urine. A plot of drug remaining to be excreted in urine (Figure 5D) allows estimation of an elimination rate constant by fitting a straight line to the central portion of the curve that corresponds to a period following completion of drug distribution during which elimination is exponential. The value of 0.051 min^{-1} compares favourably with the value calculated for β from plasma data of 0.034 min^{-1}. An estimate for CL_R of 3.2 ml min^{-1} was also obtained from the

Table 3

Pharmacokinetic (PK) constants obtained from analyses of plasma drug concentrations following intravenous (IV) administration of different drug doses under conditions of varied clearance, with the simulator in a one-compartment configuration (see Figure 3)

Figure 3A					
LIVER pump setting		**3 ml min^{-1}**		**12 ml min^{-1}**	
KIDNEY 1 pump setting		**3 ml min^{-1}**		**4 ml min^{-1}**	
KIDNEY 2 pump setting		**4 ml min^{-1}**		**3 ml min^{-1}**	
Acute IV Administration		**Dose:** 0.96 mg			
PK parameter	**Equation/method used**	**● SLOW**	**PK Solver**	**▲ FAST**	**PK Solver**
C_{t0}	Single-phase exponential decay fit	10.7 mg l^{-1}	10.7 mg l^{-1}	10.6 mg l^{-1}	10.8 mg l^{-1}
k	Single-phase exponential decay fit	0.077 min^{-1}	0.075 min^{-1}	0.179 min^{-1}	0.184 min^{-1}
$t_{1/2}$	Single-phase exponential decay fit	9.0 min	9.2 min	3.9 min	3.8 min
AUC_{IV}	Equation (3); Table 1; AUC = C_{t0} / k	138 min × mg l^{-1}	141 min × mg l^{-1}	59.4 min × mg l^{-1}	58.5 min × mg l^{-1}
V_D	Equation (1); Table 1; V_D = Dose / C_{t0}	89.9 ml	89.9 ml	90.5 ml	89.1 ml
CL_{Total}	Equation (2); Table 1; CL_{Total} = Dose / AUC	6.9 ml min^{-1}	6.8 ml min^{-1}	16.2 ml min^{-1}	16.4 ml min^{-1}
r^2	Single-phase exponential decay fit	0.9994	0.999	0.9978	0.999
Figure 3B					
PK parameter	**Equation/method used**	**● SLOW**		**▲ FAST**	
Y-intercept	Linear regression fit	1.02		1.06	
C_{t0}	$10^{Y\text{–intercept}}$	10.4 mg l^{-1}		11.5 mg l^{-1}	
slope	Linear regression fit	–0.032		–0.085	
k	Equation (6); Table 1; –k = slope × 2.303	0.074 min^{-1}		0.195 min^{-1}	
$t_{1/2}$	Equation (7); Table 1; $t_{1/2}$ = 0.693 / k	9.4 min		3.6 min	
r^2	Linear regression fit	0.9993		0.9975	
Figure 3C					
LIVER pump setting		**12 ml min^{-1}**			
KIDNEY 1 pump setting		**4 ml min^{-1}**			
KIDNEY 2 pump setting		**3 ml min^{-1}**			
Acute IV Administration		**Dose:** 0.96 mg		**Dose:** 0.32 mg	
PK parameter	**Equation/method used**	**▲ 0.96 mg**	**PK Solver**	**▼ 0.32 mg**	**PK Solver**
C_{t0}	Single-phase exponential decay fit	10.6 mg l^{-1}	10.8 mg l^{-1}	3.6 mg l^{-1}	3.7 mg l^{-1}
k	Single-phase exponential decay fit	0.179 min^{-1}	0.184 min^{-1}	0.184 min^{-1}	0.191 min^{-1}
$t_{1/2}$	Single-phase exponential decay fit	3.9 min	3.8 min	3.8 min	3.6 min
AUC_{IV}	Equation (3); Table 1; AUC = C_{t0} / k	59.4 min × mg l^{-1}	58.5 min × mg l^{-1}	19.9 min × mg l^{-1}	19.5 min × mg l^{-1}
V_D	Equation (1); Table 1; V_D = Dose / C_{t0}	90.5 ml	89.1 ml	89.9 ml	85.7 ml
CL_{Total}	Equation (2); Table 1; CL_{Total} = Dose / AUC	16.2 ml min^{-1}	16.4 ml min^{-1}	16.1 ml min^{-1}	16.4 ml min^{-1}
r^2	Single-phase exponential decay fit	0.9978	0.999	0.9964	0.999
Figure 3D					
PK parameter	**Equation/method used**	**▲ 0.96 mg**		**▼ 0.32 mg**	
Y-intercept	Linear regression fit	1.06		0.57	
C_{t0}	$10^{Y\text{–intercept}}$	11.5 mg l^{-1}		3.71 mg l^{-1}	
slope	Linear regression fit	–0.085		–0.085	
k	Equation (6); Table 1; –k = slope × 2.303	0.195 min^{-1}		0.196 min^{-1}	
$t_{1/2}$	Equation (7); Table 1; $t_{1/2}$ = 0.693 / k	3.6 min		3.6 min	
r^2	Linear regression fit	0.9975		0.9965	

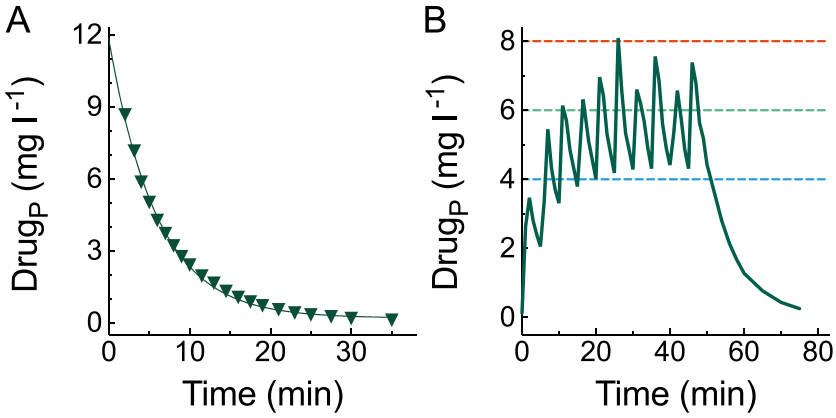

Figure 4

Single (A) and repeated (B) intravenous dosing in a one-compartment configuration. Pharmacokinetic parameters (see Table 4) were calculated based upon results from the single-dose experiment shown in (A) and were used to calculate repeated dosing parameters that would maintain steady-state concentration at approximately 6 mg l^{-1} (▬▬) and within a range between 4 (▬▬) and 8 mg l^{-1} (▬▬) (B). HEART pump: 132 ml min^{-1}, LIVER pump: 7 ml min^{-1}, KIDNEY 1 pump: 4 ml min^{-1}, KIDNEY 2 pump: 3 ml min^{-1}

Table 4

Pharmacokinetic (PK) constants obtained from analyses of plasma samples from single and repeated intravenous (IV) dosing experiments, with the simulator in a one-compartment configuration (see Figure 4)

Figure 4A			
LIVER pump setting **KIDNEY 1 pump setting** **KIDNEY 2 pump setting** **Drug dose:** 0.96 mg		**7 ml min^{-1}** **4 ml min^{-1}** **3 ml min^{-1}** **Acute IV Administration**	
PK parameter	**Equation/method used**	**▼ IV**	**PK Solver**
C_{t0}	Single-phase exponential decay fit	11.8 mg l^{-1}	12.0 mg l^{-1}
k	Single-phase exponential decay fit	0.169 min^{-1}	0.131 min^{-1}
$t_{1/2}$	Single-phase exponential decay fit	4.1 min	5.3 min
V_D	Equation (1); Table 1; V_D = Dose / C_{t0}	81.1 ml	95.4 ml
CL_{Total}	Equation (2); Table 1; CL_{Total} = Dose / AUC	13.7 ml min^{-1}	12.5 ml min^{-1}
r^2	Single-phase exponential decay fit	0.9978	0.9985
Figure 4B			
PK parameter	**Equation/method used**	▬▬	
Maintenance dose rate	Equation (12); Table 1; Maintenance dose rate = $C_{SS} \times V_D \times k_{el}$	0.082 mg min^{-1}	
τ	Equation (13); Table 1; C_{max}: 8 mg l^{-1}, C_{min}: 4 mg l^{-1}	5 min	
Total Dose/5 min	Total dose = maintenance dose rate (mg min^{-1}) × 5 (min)	0.41 mg	

fraction of the total dose eliminated in the urine; this rate is similar to the nominal KIDNEY 1 pump setting of 3 ml min^{-1}.

In addition to oral bioavailability (*vide supra*), PO administration of drug allows determination of parameters such as C_{max} (the highest drug concentration observed in the plasma) and t_{max} (the time at which C_{max} is observed) [17]. Further, with the apparatus in a two-compartment configuration, terminal $t_{½}$ (half-life, influenced by absorption, distribution and elimination) can be determined [17]. Figure 6 and Table 6 illustrate the effects of ORAL BIOAVAILABILITY pump rate and stomach volume on parameters associated with PO administration.

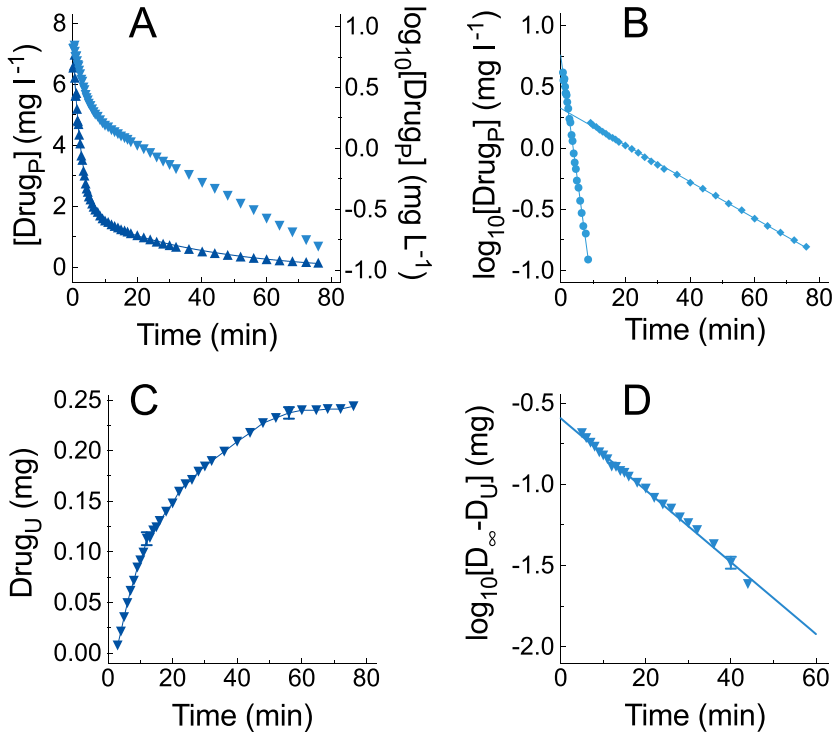

Figure 5

Two-compartment modelling of plasma and urinary drug concentrations following intravenous administration. Calculated pharmacokinetic parameters are shown in Table 5. (A) Plasma data fitted with a two-phase exponential decay equation, plotted on linear (▲) or logarithmic (▼) Y-axes. (B) Results from a classical manual analysis of logarithmic data in (A), by the method of residuals, separating and defining the contributions of distribution (●) and elimination (◆) to the two-compartment hockey-stick profile. (C) Appearance of drug in the urine provides an estimate for D_∞ from the plateau of 0.24 mg. (D) Analysis of urinary data by the sigma-minus method followed by linear regression analysis yields an elimination rate constant, k, of 0.051 min^{-1}. HEART pump: 132 ml min^{-1}, LIVER pump: 7 ml min^{-1}, TISSUE pump: 9 ml min^{-1}, KIDNEY 1: 3 ml min^{-1}, KIDNEY 2: 4 ml min^{-1}, TISSUE compartment: 100 ml

Table 5

Pharmacokinetic (PK) constants obtained from analyses of plasma and urinary drug concentrations following intravenous (IV) administration, with the simulator in a two-compartment configuration (see Figure 5)

Figure 5A		
Liver pump setting **KIDNEY 1 pump setting; KIDNEY 2 pump setting** **TISSUE pump setting; tissue compartment** **Drug dose:** 0.96 mg		**7 ml min^{-1}** **3 ml min^{-1}; 4 ml min^{-1}** **9 ml min^{-1}; 100 ml** **Acute IV Administration**
PK parameter	**Equation/method used**	**▲ (linear Y-axis)**
C_{t0}	Two-phase exponential decay fit	7.57 mg l^{-1}
k_{dist}	Two-phase exponential decay fit	0.38 min^{-1}
$t_{1/2\ dist}$	Two-phase exponential decay fit	1.8 min
k_{el}	Two-phase exponential decay fit	0.026 min^{-1}
$t_{1/2\ el}$	Two-phase exponential decay fit	26.6 min
AUC_{IV}	Equation (3); Table 1; AUC = C_{t0} / k	75.3 min × mg l^{-1}
$V_{D\ SS}$	Equation (9); Table 1; $V_{D\ SS}$ = (Dose × (A / α^2 + B / β^2)) / AUC^2	307 ml
$V_{D\ Area}$	Equation (10); Table 1; $V_{D\ Area}$ = Dose / (AUC × β)	370 ml
$V_{D\ Extrap}$	Equation (11); Table 1; $V_{D\ Extrap}$ = Dose / B-intercept	453 ml
CL_{Total}	Equation (2); Table 1; CL_{Total} = Dose / AUC	12.8 ml min^{-1}
r^2	Two-phase exponential decay fit	0.9948

(*continues*)

Table 5

(Continued)

Figure 5B			
PK parameter	**Equation/method used**	◆	**PK Solver**
Y-intercept	Linear regression fit	0.326	
B	$10^{Y-intercept}$	2.12 mg l^{-1}	1.92 mg l^{-1}
slope	Linear regression fit	–0.015	
k_{el} or β	Equation (6); Table 1; –k = slope × 2.303	0.034 min^{-1}	0.032 min^{-1}
$t_{1/2\ el}$	Equation (7); Table 1; $t_{1/2}$ = 0.693 / k	20.1 min	22.0 min
r^2	Linear regression fit	0.9992	
PK parameter	**Equation/method used**	●	**PK Solver**
Y-intercept	Linear regression fit	0.76	
A	$10^{Y-intercept}$	5.75 mg l^{-1}	5.52 mg l^{-1}
slope	Linear regression fit	–0.196	
k_{dist} or α	Equation (6); Table 1; –k = slope × 2.303	0.45 min^{-1}	0.38 min^{-1}
$t_{1/2\ dist}$	Equation (7); Table 1; $t_{1/2}$ = 0.693 / k	1.5 min	1.8 min
r^2	Linear regression fit	0.9952	
k_{12}	Equation (14); Table 1; $k_{12} = \frac{AB(\beta-\alpha)^2}{(A+B)(A\beta+B\alpha)}$	0.23 min^{-1}	0.20 min^{-1}
k_{21}	Equation (15); Table 1; $k_{21} = \frac{(A\beta+B\alpha)}{A+B}$	0.15 min^{-1}	0.12 min^{-1}
k_{10}	Equation (16); Table 1; $k_{10} = \frac{\alpha\beta(A+B)}{(A\beta+B\alpha)}$	0.10 min^{-1}	0.099 min^{-1}
Figures 5C & 5D			
PK parameter	**Equation/method used**	▼	
plateau (D_∞)	Average of last three data points	0.242 mg	
PK parameter	**Equation/method used**	▼	
slope	(D_∞-D_U) Nonlinear regression fit	–0.0221	
k	Equation (6); Table 1; –k = slope × 2.303	0.051 min^{-1}	
$t_{1/2}$	Equation (7); Table 1; $t_{1/2}$ = 0.693 / k	13.6 min	
CL_R	Equation (8); Table 1; CL_R = (Plateau / Total Dose) × CL_{Total}	3.2 ml min^{-1}	
r^2	(D_∞-D_U) Nonlinear regression fit	0.9907	

A, intercept with log Y-axis of extrapolated distribution phase; B, intercept with log Y-axis of extrapolated elimination phase; k_{dist}, first order rate constant for distribution; $t_{1/2\ dist}$, half life for drug distribution; $t_{1/2\ el}$, half life for drug elimination

Figure 6A shows how the ORAL BIOAVAILABILITY pump mimics first-pass metabolism; values for oral bioavailability (F) measured in these experiments (67% and 32%) were consistent with target values of 70% and 30%, confirming the robustness of the approach. Figure 6B shows semilogarithmic plots of those data from Figure 6A obtained after absorption and distribution were complete. Despite the programmed differences in oral bioavailability, similarities in k and $t_{½}$ values are consistent with identical LIVER and KIDNEY 1 pump settings in these experiments. As the ORAL BIOAVAILABILITY pump rate increased, the calculated B-intercept also decreased in a manner consistent with the degree to which drug was lost to first pass metabolism.

The stomach contains a constant volume of water (Figure 1 , component C), which may be varied between around 5 and 50 ml prior to beginning an experiment, thereby influencing the rate at which drug moves from the stomach into the systemic circulation. Figure 6C shows concentration–time profiles following a single PO dose of 0.96 mg drug, with stomach volumes of 45, 25 and 5 ml. Higher stomach volumes result in a lower C_{max} and a slightly longer t_{max}, with a small reduction in AUC (Table 6). Semilogarithmic plots of the elimination phases of these data (Figure 6D) indicate similar B-intercepts and slopes, confirming that the predominant effect of increasing the stomach volume is to reduce the rate of absorption and smooth the concentration–time profile, mimicking a sustained-release oral preparation.

Varying the volume of water present in the tissue compartment bottle (Figure 1, component N) allows the user to model two-compartment drugs with different volumes of distribution. Figure 7 shows plots of distribution and elimination phases, obtained by curve-stripping of data from experiments in which drug was administered IV to a system with tissue compartment volumes of 100, 200 and 500 ml. Table 7 lists the calculated parameters. Analyses reveal that, as expected, both the half-lives for drug distribution ($t_{½\ dist}$) and elimination ($t_{½\ el}$) values increase with increasing tissue compartment volume, while the B-intercept

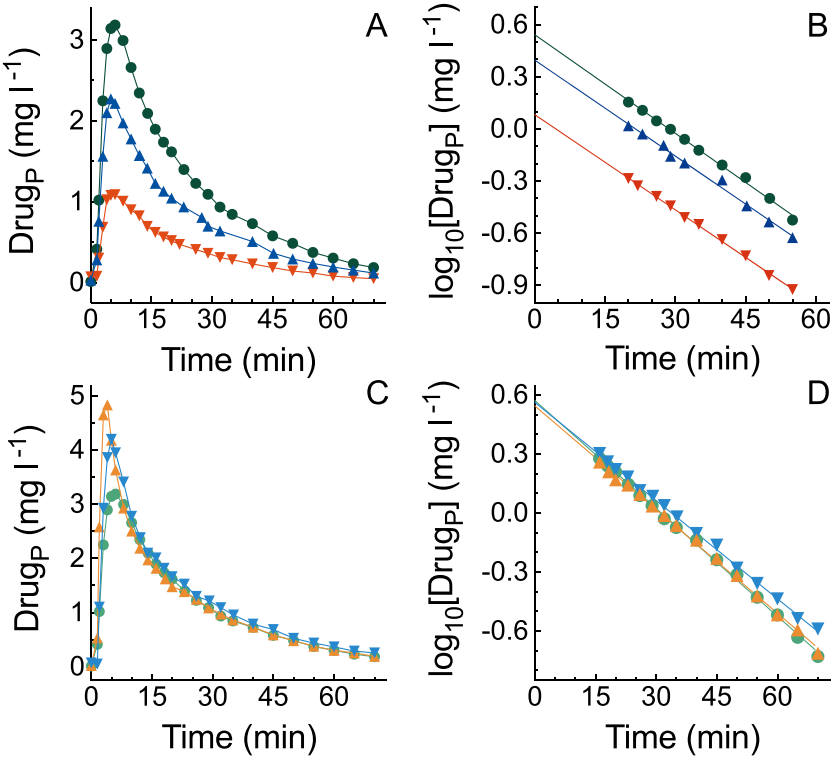

Figure 6

Effects of varying oral bioavailability or stomach volume on plasma concentration–time profiles following oral administration in a two-compartment configuration. Calculated pharmacokinetic parameters are shown in Table 6. (A) Effects of ORAL BIOAVAILABILITY pump rates on plasma concentration–time profiles. Rates of 0 (●), 5 (▲) and 24 ml min^{-1} (▼) were chosen to model bioavailabilities of 100, 70 and 30%, respectively. (B) Semilogarithmic plots of the elimination phase data, following absorption and distribution, shown in (A), reveal parallel lines, confirming that pharmacokinetic parameters associated with elimination are unaffected by modifying bioavailability. (C) Effect of initial stomach volume on peak concentration of drug in plasma and the time required to reach peak concentration. Water volumes initially present in the stomach were 45 ml (●), 25 ml (▼) and 5 ml (▲). (D) Semilogarithmic plots of the elimination phase data, following absorption and distribution, shown in (C), reveal parallel overlapping lines, confirming that effects of changing stomach volume are limited to those on rate of absorption. HEART pump: 132 ml min^{-1}, LIVER pump: 7 ml min^{-1}, TISSUE pump: 12 ml min^{-1}, KIDNEY 1: 3 ml min^{-1}, KIDNEY 2: 4 ml min^{-1}

value falls, consistent with increasing V_D values. Calculated values for microconstants for intercompartmental transfer also reflect differences in the volume of the tissue compartment.

With the apparatus configured for two-compartment kinetics, the TISSUE pump was set to 3, 7 or 17 ml min^{-1} while the dose of methylene blue, all other pump rate settings, and the tissue compartment volume, were kept constant. Figure 8 shows plots following curve-stripping of data obtained. As expected, calculated values for k_{12} and k_{21} were smaller at the lower pump settings, while k_{10} remained largely independent of the TISSUE pump rate (Table 8). Not surprisingly, the half-lives for both distribution and elimination were shorter with faster transfer of drug between compartments (Table 8).

With knowledge of PK parameters calculated from data obtained from acute IV (and, if necessary, PO) dosing experiments, dosing conditions for chronic (repeated or infusion) dosing, as well as loading dose requirements, may be determined (see Table 1). Figure 9 illustrates concentration–time profiles from an acute IV study, and from several subsequent chronic IV (injection and infusion) experiments, as well as chronic PO dosing experiments, completed under conditions similar to those used for the initial acute IV study. For chronic PO dosing experiments, the ORAL BIOAVAILABILITY pump was not turned on, such that F was 100%. The objective in each chronic dosing experiment was to achieve a desired mean C_{SS}.

With the apparatus configured for two-compartment kinetics, a single IV dose of 0.96 mg drug was administered, and data were collected and analysed as described above to obtain PK constants (Figure 9A and Table 9). Figure 9B shows data from a chronic PO dosing experiment (1.05 mg drug every 10 min) designed to achieve a mean C_{SS} of 6 mg l^{-1}, in which the stomach volume was 17 ml. Figure 9B (inset) shows the peak:trough ratio at steady state for the data shown in Figure 9B, and for data from a parallel experiment (not shown) in which a stomach volume of 35 ml was used. These results demonstrate the enhanced smoothing effects of increasing stomach volume, mimicking the slower absorption that might be observed with a sustained release oral preparation. Figure 9 C shows a similar experiment but with drug administered by

Table 6

Pharmacokinetic (PK) constants obtained from analyses of plasma drug concentrations following *per os* (PO) administration under conditions of varied bioavailability or stomach volume, with the simulator in a two-compartment configuration (see Figure 6)

Figure 6A				
LIVER pump setting		**7 ml min^{-1}**		
KIDNEY 1 pump setting; KIDNEY 2 pump setting		**3 ml min^{-1}; 4 ml min^{-1}**		
TISSUE pump setting; tissue compartment		**12 ml min^{-1}; 100 ml**		
Drug dose: 0.96 mg		**Acute Oral Administration**		
ORAL BIOAVAILABILITY pump setting		**0 ml min^{-1}**	**5 ml min^{-1}**	**24 ml min^{-1}**
PK parameter	**Equation/method used**	**● 100%**	**▲ 70%**	**▼ 30%**
AUC_{PO}	Equation (4); Table 1; AUC = AUC + C_{tn} / k	81.4 min × mg l^{-1}	54.5 min × mg l^{-1}	26.4 min × mg l^{-1}
F	$F = AUC_{PO} / AUC_{100} \times 100$	100%	67.0%	32.4%
Figure 6B				
PK parameter	**Equation/method used**	**● 100%**	**▲ 70%**	**▼ 30%**
Y-intercept	Linear regression fit	0.542	0.396	0.083
B	$10^{Y\text{–intercept}}$	3.49 mg l^{-1}	2.49 mg l^{-1}	1.21 mg l^{-1}
slope	Linear regression fit	–0.0189	–0.0184	–0.0183
k_{el} or β	Equation (6); Table 1; –k = slope × 2.303	0.044 min^{-1}	0.042 min^{-1}	0.042 min^{-1}
$t_{1/2\ el}$	Equation (7); Table 1; $t_{1/2} = 0.693 / k$	15.9 min	16.4 min	16.5 min
r^2	Linear regression fit	0.996	0.9925	0.9986
Figure 6C				
ORAL BIOAVAILABILITY pump setting		**0 ml min^{-1}**		
Stomach volume		**45 ml**	**25 ml**	**5 ml**
PK parameter	**Equation/method used**	●	▼	▲
AUC_{PO}	Equation (4); Table 1; $AUC = \sum AUC_{t_{n-1}}^{t_n} + C_{tn}/k$	81.5 min × mg l^{-1}	87.9 min × mg l^{-1}	93.1 min × mg l^{-1}
t_{max}	Figure 6C	6 min	5 min	4 min
C_{max}	Figure 6C	3.2 mg l^{-1}	4.2 mg l^{-1}	4.8 mg l^{-1}
Figure 6D				
PK parameter	**Equation/method used**	●	▼	▲
Y-intercept	Linear regression fit	0.572	0.562	0.544
B	$10^{Y\text{–intercept}}$	3.73 mg l^{-1}	3.65 mg l^{-1}	3.50 mg l^{-1}
slope	Linear regression fit	–0.0183	–0.0166	–0.0176
k_{el} or β	Equation (6); Table 1; –k = slope × 2.303	0.042 min^{-1}	0.038 min^{-1}	0.040 min^{-1}
$t_{1/2\ el}$	Equation (7); Table 1; $t_{1/2} = 0.693 / k$	16.5 min	18.1 min	17.1 min
r^2	Linear regression fit	0.9982	0.9986	0.998

t_{max}, time taken to reach C_{max} after a single (PO) drug dose

the IV route. Although the mean C_{SS} reached was identical, the peak:trough ratio at steady state (2.64) was markedly greater than that observed in PO experiments (Figure 9B), where smoothing due to absorption was evident.

Conventional wisdom dictates that a mean C_{SS} is typically reached after administration of drug at a constant rate for 5 half-lives of elimination (for example, Figures 9B and C). Administration of an initial loading dose avoids this delay, achieving a plasma concentration close to the target C_{SS} almost immediately. This is illustrated in Figure 9D, where the target C_{SS} of 7.4 mg l^{-1} was achieved with a PO loading dose of 2.45 mg of drug, and maintained with PO doses of 0.78 mg every 6 min. Similarly, in Figure 9E, an IV loading dose of 2.02 mg drug, and maintenance doses of 0.61 mg every 6 min, allow the target C_{SS} of 6 mg l^{-1} to be reached immediately. The initial spike observed following the IV bolus loading dose in Figure 9E is not unexpected, and is explained by the rate of administration far exceeding the rate of distribution, resulting in almost all of the larger loading dose being present initially in the central compartment.

Figure 9F illustrates a concentration–time profile obtained by infusing drug (106 μg ml^{-1}) at a constant rate of 1 ml min^{-1} via a separate infusion pump. The target C_{SS} was 6 mg l^{-1}; the plateau reached in this example

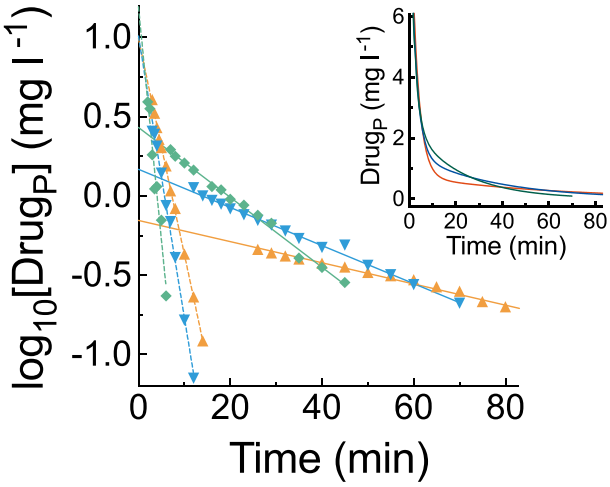

Figure 7

Effects of varying water volume in the tissue compartment bottle on plasma concentration–time profiles following intravenous administration in a two-compartment configuration. Calculated pharmacokinetic parameters are shown in Table 7. The main panel shows data from experiments with tissue compartment volumes of 100 (◆), 200 (▼) and 500 ml (▲), plotted on a logarithmic Y-axis following manual analysis by the method of residuals, with the distribution and elimination phases indicated by dashed and solid lines, respectively. Inset: raw data plotted on a linear Y-axis, obtained with tissue compartment volumes of 100 (——), 200 (——) and 500 ml (——) and fitted with a two-phase exponential decay equation. HEART pump: 132 ml min^{-1}, LIVER pump: 7 ml min^{-1}, TISSUE pump: 10 ml min^{-1}, KIDNEY 1 pump: 3 ml min^{-1}, KIDNEY 2 pump: 4 ml min^{-1}

was a little higher than the target value. Partial data sets from the infusion experiment, from 0–60 min and from 120–180 min, were fitted to two-phase association or dissociation equations, respectively. The pairs of half-lives thereby obtained were similar between the two fits, consistent with the importance of partial occupancy of transporters and enzymes involved in clearance in determining the exponential nature of the rate of drug build-up and elimination. Both exponential portions of the curve from Figure 9F are superimposed in Figure 9F (inset) in order to illustrate this point; the curves appear to be mirror images.

Student results

Students who had previously completed an undergraduate course in PK principles and calculations showed a significant improvement in their ability to answer short PK questions after attending two laboratory classes in which the simulator apparatus was used (Figure 10A). Students were also asked to score their competence in handling PK problems (Figure 10B) and their perceptions of their understanding of PK principles (Figure 10C), before and after the laboratory classes; in both categories, students self-reported a significant improvement following the laboratory classes. When asked, on a scale of 1–5 (where 1 corresponds to *strongly disagree* and 5 corresponds to *strongly agree*) whether they felt the simulator was an effective educational tool, students returned a score of 4.46 ± 0.24 (mean ± standard error of the mean, n = 13). Open-ended comments were also invited from students as part of the formal assessment of course quality conducted by the University of Alberta; these written comments, along with verbal feedback offered during and after the laboratory sessions, were overwhelmingly positive.

Table 7

Pharmacokinetic (PK) constants obtained from analyses of plasma drug concentrations following intravenous (IV) administration under conditions of varied tissue compartment volume, with the simulator in a two-compartment configuration (see Figure 7)

Figure 7				
LIVER pump setting		**7 ml min^{-1}**		
KIDNEY 1 pump setting; KIDNEY 2 pump setting		**3 ml min^{-1}; 4 ml min^{-1}**		
TISSUE pump setting		**10 ml min^{-1}**		
Drug dose: 0.96 mg		**Acute IV Administration**		
Tissue compartment		**◆ 100 ml**	**▼ 200 ml**	**▲ 500 ml**
PK parameter	**Equation/method used**	——	——	——
Y-intercept	Linear regression fit	0.432	0.168	–0.154
B	$10^{Y\text{–intercept}}$	2.70 mg l^{-1}	1.47 mg l^{-1}	0.701 mg l^{-1}
slope	Linear regression fit	–0.022	–0.012	–0.0067
k_{el} or β	Equation (6); Table 1; –k = slope × 2.303	0.051 min^{-1}	0.028 min^{-1}	0.015 min^{-1}
$t_{1/2\ el}$	Equation (7); Table 1; $t_{1/2}$ = 0.693 / k	13.7 min	25.1 min	45.1 min
r^2	Linear regression fit	0.9936	0.9919	0.9891
PK parameter	**Equation/method used**	-----	-----	-----
Y-intercept	Linear regression fit	1.19	1.01	0.992
A	$10^{Y\text{–intercept}}$	15.6 mg l^{-1}	10.2 mg l^{-1}	9.8 mg l^{-1}

(*continues*)

Table 7

(Continued)

Figure 7				
LIVER pump setting		**7 ml min^{-1}**		
KIDNEY 1 pump setting; KIDNEY 2 pump setting		**3 ml min^{-1}; 4 ml min^{-1}**		
TISSUE pump setting		**10 ml min^{-1}**		
Drug dose: 0.96 mg		**Acute IV Administration**		
Tissue compartment		◆ **100 ml**	▼ **200 ml**	▲ **500 ml**
slope	Linear regression fit	–0.293	–0.177	–0.136
k_{dist} or α	Equation (6); Table 1; –k = slope × 2.303	0.68 min^{-1}	0.41 min^{-1}	0.31 min^{-1}
$t_{1/2\ dist}$	Equation (7); Table 1; $t_{1/2}$ = 0.693 / k	1.0 min	1.7 min	2.2 min
r^2	Linear regression fit	0.957	0.9948	0.9992
k_{12}	Equation (14); Table 1; $k_{12} = \frac{AB(\beta-\alpha)^2}{(A+B)(A\beta+B\alpha)}$	0.34 min^{-1}	0.21 min^{-1}	0.16 min^{-1}
k_{21}	Equation (15); Table 1; $k_{21} = \frac{(A\beta+B\alpha)}{A+B}$	0.14 min^{-1}	0.076 min^{-1}	0.036 min^{-1}
k_{10}	Equation (16); Table 1; $k_{10} = \frac{\alpha\beta(A+B)}{(A\beta+B\alpha)}$	0.24 min^{-1}	0.15 min^{-1}	0.13 min^{-1}
PK parameter	**Equation/method used**			
C_{t0}	Two-phase exponential decay fit	11.0 mg l^{-1}	11.0 mg l^{-1}	11.9 mg l^{-1}
k_{dist}	Two-phase exponential decay fit	0.49 min^{-1}	0.40 min^{-1}	0.34 min^{-1}
$t_{1/2\ dist}$	Two-phase exponential decay fit	1.4 min	1.7 min	2.0 min
k_{el}	Two-phase exponential decay fit	0.047 min^{-1}	0.028 min^{-1}	0.017 min^{-1}
$t_{1/2\ el}$	Two-phase exponential decay fit	14.8 min	24.3 min	41.2 min
AUC	Equation (4); Table 1; $AUC = \sum AUC_{t_{n-1}}^{t_n} + C_{tn}/k$	72.0 min × mg l^{-1}	77.2 min × mg l^{-1}	78.6 min × mg l^{-1}
$V_{D\ SS}$	Equation (9); Table 1; $V_{D\ SS}$ = (Dose × (A / α^2 + B / β^2)) / AUC^2	201 ml	319 ml	477 ml
$V_{D\ Area}$	Equation (10); Table 1; $V_{D\ Area}$ = Dose / (AUC × β)	263 ml	449 ml	794 ml
$V_{D\ Extrap}$	Equation (11); Table 1; $V_{D\ Extrap}$ = Dose / B-intercept	355 ml	652 ml	1369 ml
CL_{Total}	Equation (2); Table 1; CL_{Total} = Dose / AUC	13.3 ml min^{-1}	12.4 ml min^{-1}	12.2 ml min^{-1}
r^2	Two-Phase Exponential Decay Fit	0.9961	0.9923	0.9989

Figure 7 PK Solver Values				
Tissue compartment		**100 ml**	**200 ml**	**500 ml**
PK parameter	**Equation/method used**	◆	▼	▲
AUC	PK solver compartmental analysis	74.6 min × mg l^{-1}	76.5 min × mg l^{-1}	77.7 min × mg l^{-1}
$V_{D\ SS}$		179 ml	315 ml	619 ml
k_{el} or β		0.051 min^{-1}	0.028 min^{-1}	0.012 min^{-1}
$t_{1/2\ el}$		13.7 min	24.3 min	56.8 min
B		2.57 mg l^{-1}	1.51 mg l^{-1}	0.56 mg l^{-1}
k_{dist} or α		0.65 min^{-1}	0.40 min^{-1}	0.26 min^{-1}
$t_{1/2\ dist}$		1.1 min	1.7 min	2.7 min
A		15.5 mg l^{-1}	9.5 mg l^{-1}	8.2 mg l^{-1}
k_{12}		0.32 min^{-1}	0.21 min^{-1}	0.13 min^{-1}
k_{21}		0.14 min^{-1}	0.080 min^{-1}	0.028 min^{-1}
k_{10}		0.24 min^{-1}	0.14 min^{-1}	0.11 min^{-1}

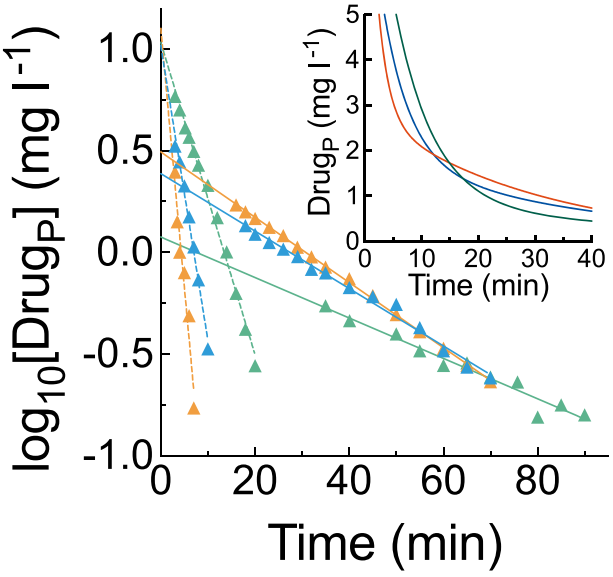

Figure 8

Effects of varying TISSUE PUMP rate on plasma concentration–time profiles following intravenous administration in a two-compartment configuration. Calculated pharmacokinetic parameters are shown in Table 8. The main panel shows data from experiments with pump settings of 3 (▲), 7 (▲) and 17 ml min^{-1} (▲), with a fixed tissue compartment volume of 100 ml. Data are plotted on a logarithmic Y-axis following manual analysis by the method of residuals, with the distribution and elimination phases indicated by dashed and solid lines, respectively. (Inset: raw data plotted on a linear Y-axis, obtained with TISSUE PUMP settings of 3 (——), 7 (——) and 17 ml min^{-1} (——) and fitted with a two-phase exponential decay equation). HEART pump: 132 ml min^{-1}, LIVER pump: 7 ml min^{-1}, KIDNEY 1 pump: 3 ml min^{-1}, KIDNEY 2 pump: 4 ml min^{-1}

Monitoring in real time

An optional modification to the apparatus allows for continuous spectrophotometric measurement of absorbance in a flow-through cuvette, output projected onto a screen facilitating live demonstrations of PK behaviour to larger audiences. Figure 11 illustrates examples of real-time output from a spectrophotometer following single and repeated PO and IV doses of methylene blue. With the apparatus configured for one-compartment kinetics, single IV and PO doses were administered with oral bioavailability at 100% or 60% (Figure 11A). The initial fluctuations in the IV trace reflect a duration for mixing of the bolus injection within the central compartment approximating five circuits of the water around the systemic circulation tubing. Under similar one-compartment conditions, repeated IV injections were administered to achieve a C_{SS}, and with oral bioavailability set to 60%, repeated oral doses were then administered in an attempt to achieve a similar C_{SS} (Figure 11B). Intermittent IV infusion protocols are often used to administer antibiotics when high peak concentrations associated with bolus injections may be harmful to patients [20]; one such protocol for a one-compartment drug is illustrated in Figure 11C. Finally, Figure 11D shows output following a single IV injection with the apparatus configured for two-compartment kinetics; the same data are also shown plotted on a logarithmic axis, revealing a classical *hockey-stick* curve.

Discussion and conclusions

Half of all prescribing errors are potentially preventable, and many studies have concluded that these errors are often a result of physicians' limited knowledge of pharmacology and

Table 8

Pharmacokinetic (PK) constants obtained from analyses of plasma drug concentrations following intravenous (IV) administration under conditions of varied rates of intercompartmental drug transfer, with the simulator in a two-compartment configuration (see Figure 8)

Figure 8				
LIVER pump setting		**7 ml min^{-1}**		
KIDNEY 1 pump setting; KIDNEY 2 pump setting		**3 ml min^{-1}; 4 ml min^{-1}**		
Tissue compartment		**100 ml**		
Drug dose: 0.96 mg		**Acute IV Administration**		
TISSUE pump setting		▲ **3 ml min^{-1}**	▲ **7 ml min^{-1}**	▲ **17 ml min^{-1}**
PK parameter	**Equation/method used**	——	——	——
Y-intercept	Linear regression fit	0.076	0.39	0.49
B	$10^{Y\text{–intercept}}$	1.19 mg l^{-1}	2.44 mg l^{-1}	3.12 mg l^{-1}
slope	Linear regression fit	–0.0099	–0.014	–0.016
k_{el} or β	Equation (6); Table 1; –k = slope × 2.303	0.022 min^{-1}	0.032 min^{-1}	0.037 min^{-1}
$t_{1/2\ el}$	Equation (7); Table 1; $t_{1/2}$ = 0.693 / k	30.3 min	21.3 min	18.7 min
r^2	Linear regression fit	0.96	0.9896	0.9992
PK parameter	**Equation/method used**	- - - - -	- - - - -	- - - - -
Y-intercept	Linear regression fit	1.03	1.02	1.1

(*continues*)

Table 8

(Continued)

Figure 8				
LIVER pump setting		**7 ml min^{-1}**		
KIDNEY 1 pump setting; KIDNEY 2 pump setting		**3 ml min^{-1}; 4 ml min^{-1}**		
Tissue compartment		**100 ml**		
Drug dose: 0.96 mg		**Acute IV Administration**		
TISSUE pump setting		**▲ 3 ml min^{-1}**	**▲ 7 ml min^{-1}**	**▲ 17 ml min^{-1}**
A	$10^{Y\text{–intercept}}$	10.8 mg l^{-1}	10.4 mg l^{-1}	12.6 mg l^{-1}
slope	Linear regression fit	–0.077	–0.14	–0.25
k_{dist} or α	Equation (6); Table 1; –k = slope × 2.303	0.17 min^{-1}	0.33 min^{-1}	0.58 min^{-1}
$t_{1/2\ dist}$	Equation (7); Table 1; $t_{1/2}$ = 0.693 / k	3.9 min	2.1 min	1.2 min
r^2	Linear regression fit	0.9924	0.9893	0.9513
k_{12}	Equation (14); Table 1; $k_{12} = \frac{AB(\beta-\alpha)^2}{(A+B)(A\beta+B\alpha)}$	0.057 min^{-1}	0.16 min^{-1}	0.33 min^{-1}
k_{21}	Equation (15); Table 1; $k_{21} = \frac{(A\beta+B\alpha)}{A+B}$	0.038 min^{-1}	0.090 min^{-1}	0.14 min^{-1}
k_{10}	Equation (16); Table 1; $k_{10} = \frac{\alpha\beta(A+B)}{(A\beta+B\alpha)}$	0.10 min^{-1}	0.12 min^{-1}	0.15 min^{-1}
PK parameter	**Equation/method used**			
C_{t0}	Two-phase exponential decay fit	10.4 mg l^{-1}	10.2 mg l^{-1}	13.7 mg l^{-1}
k_{dist}	Two-phase exponential decay fit	0.15 min^{-1}	0.26 min^{-1}	0.61 min^{-1}
$t_{1/2\ dist}$	Two-phase exponential decay fit	4.7 min	2.6 min	1.1 min
k_{el}	Two-phase exponential decay fit	0.018 min^{-1}	0.030 min^{-1}	0.035 min^{-1}
$t_{1/2\ el}$	Two-phase exponential decay fit	38.8 min	23.5 min	19.7 min
AUC	Equation (4); Table 1; $AUC = \sum AUC_{t_{n-1}}^{t_n} + C_{tn}/k$	111 min × mg l^{-1}	104 min × mg l^{-1}	103 min × mg l^{-1}
$V_{D\ SS}$	Equation (9); Table 1; $V_{D\ SS}$ = [Dose × (A / α^2 + B / β^2)] / AUC^2	202 ml	214 ml	210 ml
$V_{D\ Area}$	Equation (10); Table 1; $V_{D\ Area}$ = Dose / (AUC × β)	376 ml	285 ml	252 ml
$V_{D\ Extrap}$	Equation (11); Table 1; $V_{D\ Extrap}$ = Dose / B-intercept	806 ml	393 ml	307 ml
CL_{Total}	Equation (2); Table 1; CL_{Total} = Dose / AUC	8.6 ml min^{-1}	9.2 ml min^{-1}	9.3 ml min^{-1}
r^2	Two-Phase Exponential Decay Fit	0.9993	0.9979	0.9994
Figure 8 PK solver values				
Distribution pump setting		**3 ml min^{-1}**	**7 ml min^{-1}**	**17 ml min^{-1}**
PK parameter	**Equation/method used**	▲	▲	▲
AUC	PK solver compartmental analysis	113 min × mg l^{-1}	107 min × mg l^{-1}	102 min × mg l^{-1}
$V_{D\ SS}$		235 ml	266 ml	224 ml
k_{el} or β		0.018 min^{-1}	0.024 min^{-1}	0.035 min^{-1}
$t_{1/2\ el}$		38.7 min	28.3 min	19.8 min
B		0.86 mg l^{-1}	1.81 mg l^{-1}	2.96 mg l^{-1}
k_{dist} or α		0.15 min^{-1}	0.20 min^{-1}	0.60 min^{-1}
$t_{1/2\ dist}$		4.73 min	3.37 min	1.15 min
A		9.52 mg l^{-1}	6.83 mg l^{-1}	10.7 mg l^{-1}
k_{12}		0.044 min^{-1}	0.087 min^{-1}	0.35 min^{-1}
k_{21}		0.028 min^{-1}	0.062 min^{-1}	0.16 min^{-1}
k_{10}		0.092 min^{-1}	0.081 min^{-1}	0.13 min^{-1}

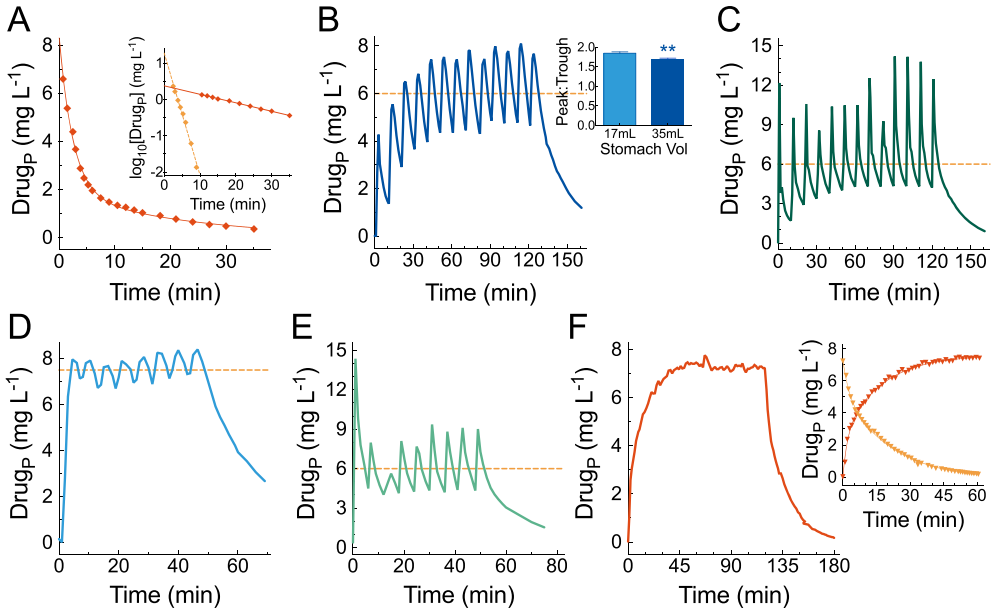

Figure 9

Repeated or chronic drug administration, with or without a loading dose, by intravenous (IV) and *per os* (PO) routes in a two-compartment configuration. Calculated pharmacokinetic parameters are shown in Table 9. (A) Main panel: Plasma data fitted with a two-phase exponential decay equation, plotted on a linear Y-axis, following a single bolus IV injection. (Inset: data plotted on a logarithmic Y-axis following manual analysis by the method of residuals, illustrating the distribution (◆) and elimination (◆) phases). Pharmacokinetic parameters calculated from this experiment were used to calculate repeated dosing parameters for experiments shown in panels B-F, completed with the apparatus in a similar configuration. (B) Repeated PO dosing of 1.05 mg drug every 10 min, calculated to achieve a C_{SS} of 6 mg l^{-1} (– – –). (Inset: peak:trough ratios at steady state from the experiment shown in the main panel (stomach volume 17 ml) and from a similar parallel experiment in which the stomach volume was 35 ml). (C) Repeated IV dosing of 1.05 mg drug every 10 min, calculated to achieve a steady-state concentration (C_{SS}) of 6 mg l^{-1} (– – –), under similar conditions used to obtain data shown in panel (B). (D) PO loading dose of 2.45 mg drug followed by repeated PO doses of 0.78 mg every 6 min, with a stomach volume of 35 ml, calculated to achieve a C_{SS} of 7.4 mg l^{-1} (– – –). (E) IV loading dose of 2.02 mg drug followed by repeated IV doses of 0.61 mg every 6 min, calculated to achieve a C_{SS} of 6 mg l^{-1} (– – –). (F) Continuous IV infusion (1 ml min^{-1} and 106 μg min^{-1}) calculated to achieve a C_{SS} of 6 mg l^{-1}. (Inset: Superimposed data from the first (▼) and last (▼) 60 min of the IV infusion shown in the main figure). HEART pump: 132 ml min^{-1}, LIVER pump: 10 ml min^{-1}, TISSUE pump: 12 ml min^{-1}, KIDNEY 1 pump: 3 ml min^{-1}, KIDNEY 2 pump: 4 ml min^{-1}, TISSUE COMPARTMENT: 100 ml

Table 9

Pharmacokinetic (PK) constants obtained from analyses of plasma drug concentrations following repeated intravenous (IV) and *per os* (PO) administration, with or without a loading dose, with the simulator in a two-compartment configuration (see Figure 9)

Figure 9A		
LIVER pump setting		**10 ml min^{-1}**
KIDNEY 1 pump setting; KIDNEY 2 pump setting		**3 ml min^{-1}; 4 ml min^{-1}**
TISSUE pump setting; tissue compartment volume		**12 ml min^{-1}; 100 ml**
Drug dose: 0.96 mg		**Acute IV Administration**
PK parameter	**Equation/method used**	◆
C_{t0}	Two-phase exponential decay fit	8.48 mg l^{-1}
k_{dist}	Two-phase exponential decay fit	0.40 min^{-1}
$t_{1/2\ dist}$	Two-phase exponential decay fit	1.7 min
k_{el}	Two-phase exponential decay fit	0.043 min^{-1}
$t_{1/2\ el}$	Two-phase exponential decay fit	16.0 min
AUC	Equation (4); Table 1; AUC = $\sum AUC_{t_{n-1}}^{t_n} + C_{tn}/k$	58.9 min × mg l^{-1}
$V_{D\ SS}$	Equation (9); Table 1; $V_{D\ SS}$ = (Dose × (A / α^2 + B / β^2)) / AUC^2	236 ml

(*continues*)

Table 9

(Continued)

Figure 9A		
LIVER pump setting **KIDNEY 1 pump setting; KIDNEY 2 pump setting** **TISSUE pump setting; tissue compartment volume** **Drug dose:** 0.96 mg		**10 ml min^{-1}** **3 ml min^{-1}; 4 ml min^{-1}** **12 ml min^{-1}; 100 ml** **Acute IV Administration**
$V_{D\ Area}$	Equation (10); Table 1; $V_{D\ Area}$ = Dose / (AUC × β)	303 ml
$V_{D\ Extrap}$	Equation (11); Table 1; $V_{D\ Extrap}$ = Dose / B-intercept	405 ml
CL_{Total}	Equation (2); Table 1; CL_{Total} = Dose / AUC	16.3 ml min^{-1}
r^2	Two-phase exponential decay fit	0.9981
PK parameter	**Equation/method used**	
Y-intercept	Linear regression fit	0.376
B	$10^{Y\text{–intercept}}$	2.38 mg l^{-1}
slope	Linear regression fit	–0.0234
k_{el} or β	Equation (6); Table 1; –k = slope × 2.303	0.054 min^{-1}
$t_{1/2\ el}$	Equation (7); Table 1; $t_{1/2}$ = 0.693 / k	12.9 min
r^2	Linear regression fit	0.9981
PK parameter	**Equation/method used**	
Y-intercept	Linear regression fit	1.28
A	$10^{Y\text{–intercept}}$	18.9 mg l^{-1}
slope	Linear regression fit	–0.336
k_{dist} or α	Equation (6); Table 1; –k = slope × 2.303	0.77 min^{-1}
$t_{1/2\ dist}$	Equation (7); Table 1; $t_{1/2}$ = 0.693 / k	0.90 min
r^2	Linear regression fit	0.9891
Figure 9B		**Repeated oral dosing**
PK parameter	**Equation/method used**	
Maintenance Dose Rate	Equation (12); Table 1; C_{SS} = 6 mg l^{-1}	0.105 mg min^{-1}
Oral Dose Rate	Equation (17); Table 1; F = 100%	0.105 mg min^{-1}
τ	Equation (13); Table 1; C_{max}:C_{min} = 1.5	10 min
Total Dose/10 min	Total dose = maintenance dose rate (mg min^{-1}) × 10 (min)	1.05 mg
Figure 9C		**Repeated IV dosing**
PK parameter	**Equation/method used**	
Maintenance dose rate	Equation (12); Table 1; C_{SS} = 6 mg l^{-1}	0.105 mg min^{-1}
τ	Equation (13); Table 1; $\frac{C_{max}\ \text{at steady state}}{C_{min}\ \text{at steady state}} = \frac{1}{e^{-k_{el}\cdot\tau}}$	10 min
Total Dose/10 min	Total dose = maintenance dose rate (mg min^{-1}) × 10 (min)	1.05 mg
Figure 9D		**Repeated oral dosing with loading dose**
PK parameter	**Equation/method used**	
Loading dose	Equation (18); Table 1; Loading Dose = C_{SS} × V_D	3.04 mg
Maintenance dose rate	Equation (12); Table 1; C_{SS} = 7.4 mg l^{-1}	0.130 mg min^{-1}
Oral dose rate	Equation (17); Table 1; F = 100%	0.130 mg min^{-1}
τ	Equation (13); Table 1; $\frac{C_{max}\ \text{at steady state}}{C_{min}\ \text{at steady state}} = \frac{1}{e^{-k_{el}\cdot\tau}}$	6 min
Total dose/6 min	Total dose = maintenance dose rate (mg min^{-1}) × 6 (min)	0.782 mg

(*continues*)

Table 9

(Continued)

Figure 9E		**Repeated IV Dosing with Loading Dose**
PK parameter	**Equation/method used**	
Loading dose	Equation (18); Table 1; Loading Dose = $C_{SS} \times V_D$	2.05 mg
Maintenance dose rate	Equation (12); Table 1; C_{SS} = 6 mg l^{-1}	0.102 mg min^{-1}
τ	Equation (13); Table 1; $\frac{C_{max} \text{ at steady state}}{C_{min} \text{ at steady state}} = \frac{1}{e^{-k_{el} \cdot \tau}}$	6 min
Total dose/6 min	Total dose = maintenance dose rate (mg min^{-1}) × 6 (min)	0.612 mg
Figure 9F		**IV Infusion**
PK parameter	**Equation/method used**	
Maintenance dose rate	Equation (12); Table 1; C_{SS} = 6 mg l^{-1}	0.105 mg min^{-1}
Total dose/h	Maintenance dose rate (mg min^{-1}) × 60 (min h^{-1})	6.31 mg h^{-1}
$t_{1/2}$ ▼	Two-phase association fit	1.30 and 11.7 min
$t_{1/2}$ ▼	Two-phase exponential decay fit	1.84 and 15.2 min

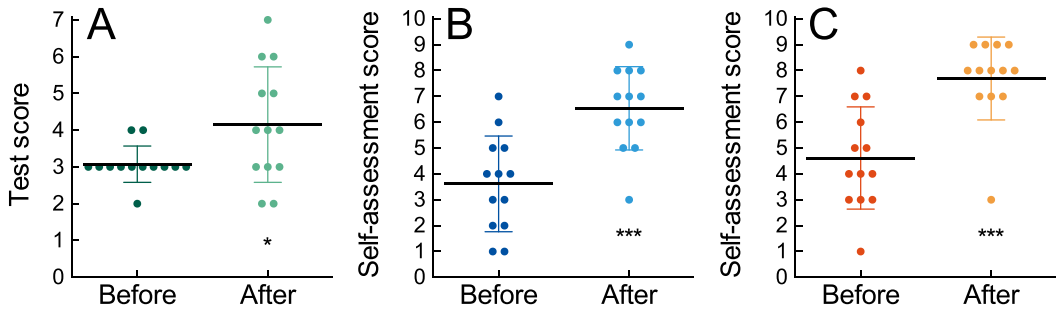

Figure 10

Scatter plots showing undergraduate student performance and self-assessment scores before and after completing two laboratory classes with the pharmacokinetics (PK) simulator. Statistical comparisons were made with Wilcoxon's matched pairs test; bars show mean ± SD (n = 13) (A) Scores obtained in a short test of ability to carry out PK calculations (* P = 0.0313). (B) Student self-reporting of perception of their own competence in dealing with the mathematical and graphing aspects of PK, before and after completing the laboratory classes (*** P = 0.0002). (C) Student self-reporting of perception of their understanding of the mathematical aspects of PK, before and after completing the laboratory classes (*** P = 0.0002)

pharmacotherapy [21–24]. While human error accounts for some of these mistakes, fundamental knowledge deficits typically underlie the more immediate causes [13]. A weak knowledge base of PK, such as misunderstanding the concept of volume of distribution, can have devastating outcomes [13, 24]. Before discussing five case studies in which human patients succumbed to hydromorphone overdoses, Lehmann stressed that 'had the fundamental principles of clinical pharmacology been properly understood, it is likely that these therapeutic misadventures would have been averted' [13].

Difficulties in understanding and applying PK principles are not restricted to medical students or doctors; those in other clinical professions such as pharmacy and nursing also struggle [3–5, 8]. Although one study reports instructional hours in pharmacology and pharmacotherapy to be around 6-fold higher for pharmacy students compared with medical students [25], increased instructional time does not necessarily translate to enhanced mastery of the subject. Clinical pharmacokinetics, one of the most difficult areas of the curriculum to teach by conventional methods, requires the use of contextual transfer strategies [4, 5].

Brackett *et al.* [5] created a PK course centred on *flipping the classroom* in order to encourage active learning techniques, such as *think–pair–share*, group discussions and problem-based learning, which resulted in noted improvements in student understanding. The use of computer programs to supplement lectures can improve problem solving ability in clinical PK [4], although this approach has limitations in terms of how students visualize abstract concepts.

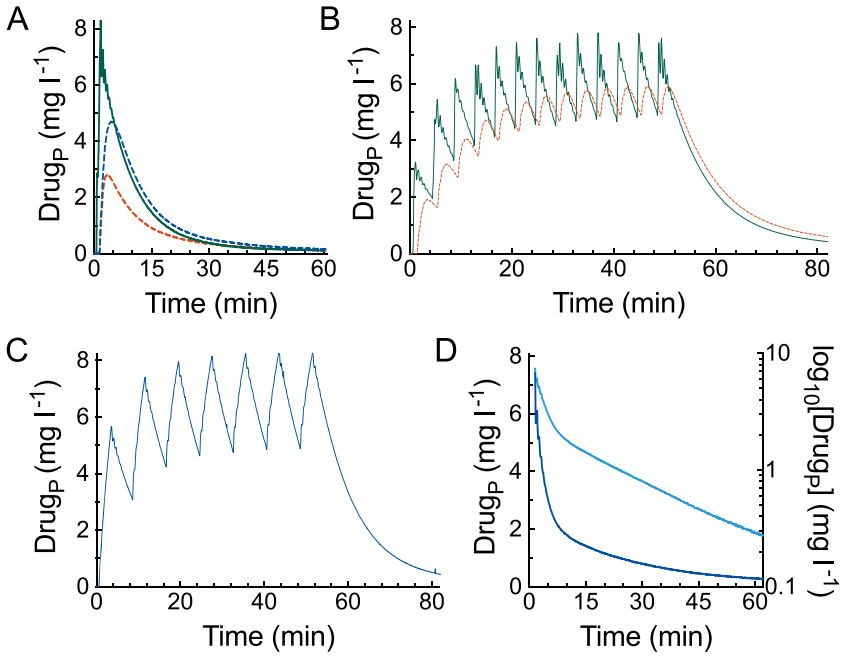

Figure 11

Examples of real-time spectrophotometer output, obtained by diverting a small portion of the systemic circulation through a flow-through cuvette, that may be projected onto a screen. (A) Single intravenous (IV; ——) and *per os* doses of 1 mg, with oral bioavailability set as 100% (– – –) or 60% (– – –), in a one-compartment configuration. (B) Repeated IV injections of 0.34 mg every 4 min (——) and repeated PO doses of 0.57 mg every 4 min with oral bioavailability set as 60% (– – –), calculated to achieve a C_{SS} of 6 mg l^{-1}. (C) Intermittent IV infusions (0.68 mg infused over 3 min, every 8 min) in a one-compartment configuration, calculated to achieve a C_{SS} of 6 mg l^{-1}. (D) Single IV injection of 1 mg, with the simulator in a two-compartment configuration, plotted on linear (——) or logarithmic (——) Y-axes

The ADAM addresses some of these concerns by allowing students, through observation and experimentation, to discover how introducing changes to the system impacts PK parameters. As such, it allows students to engage with the equations and techniques of analysis learned in lectures to formulate and evaluate drug-dosing regimens in a zero-risk environment. We have constructed five sets of apparatus for use in our teaching laboratories; these apparatuses may be programmed to model five individuals receiving doses of the same drug (offering opportunities to study interindividual variation) or to model one individual receiving doses of five different drugs (offering opportunities to explore a variety of drug behaviours). The apparatus is constructed in such a way that the pumps and tubing, mounted on a series of shelves bolted to a laboratory cart, are concealed behind a full-size human outline printed on rigid foam board. As such, drug may be administered by syringe through a cannula entering the mouth, or via an injection port on a Tygon tubing *vein* that is exposed on the patient's forearm. The sampling port is also located on the forearm vein, while urine is collected from a cannula representing the urethra that exits the inguinal region.

The apparatus was designed to mimic the *outcome* of physiological or pathological processes affecting PK behaviour, rather than to model the mechanisms that give rise to changes in PK parameters. As such, the modeller offers a realistic experience to students, since it is through analysis of plasma concentration–time data that these mechanisms are indirectly observed in real patients. For example, the consequences of a change in plasma protein binding would be observed as predictable changes in V_D, k and CL; pump rates and vessel volumes may be altered to create the changes in these parameters that would be observed in a patient where plasma protein binding had changed. Similarly, clinical situations such as renal failure, hepatic enzyme induction or metabolic drug–drug interactions are quite straightforward to depict. With PKSolver, we were able to validate the data in order to show that the outputs from the modeller are physiologically sound; parameter values calculated through classical methods were similar to those calculated with PKSolver.

It is apparent that volumes of both the central and tissue compartments are unrealistically low in the ADAM, leading to short half-lives of distribution and elimination. In this regard, the design was intentional, to facilitate collection of plasma and urine samples over a period of several half-lives within the time constraints of a single afternoon laboratory class. Should more realistic values be required, the apparatus lends itself to modification, through introduction of a large stirred central reservoir in series with the systemic circulation, and/or a much larger tissue compartment reservoir. Similarly, the apparatus may be modified to create more complex systems; for example, introduction of a second *deep tissue* compartment in parallel with the systemic circuit to create a three-compartment open model would be straightforward, and may be appropriate for students of pharmacy. However, more realistic clearance rates and volumes of distribution would preclude incorporation of repeated dosing

experiments into a half-day laboratory class and would render the apparatus largely unsuitable for in-lecture demonstration of core principles.

The only basic PK phenomenon that has proved impossible to simulate with the modeller in the configuration as described is that of zero order elimination, where, initially, a constant amount of drug is eliminated in unit time. In such a scenario, the concentration of drug in the plasma would fall linearly, rather than exponentially. While it would be straightforward to model zero order appearance of drug in the urine, simulating the concentration-independent loss of drug from the plasma has, thus far, proved unachievable.

An optional modification of the apparatus to introduce a flow-through cuvette in parallel to the systemic circulation facilitates observation of PK behaviour *in situ*. Connection of the spectrophotometer VGA output to a projector thus allows demonstration of real-time PK to an audience in a lecture hall, offering opportunities for live illustration of PK concepts in parallel with a didactic lecture. Since it is possible to achieve values for $t_{½}$ in the region of 3 min, topics such as steady-state with repeated dosing may be demonstrated within the time constraints of a 1-h lecture. New lectures planned for the medical curriculum at the University of Alberta will incorporate use of the simulator during lectures to demonstrate, for example, drug accumulation during repeated oral dosing of the simulator by a student volunteer, and the consequences for the patient of drinking grapefruit juice. Lecture slides describing governing principles will be projected onto one screen and real-time absorbance measurements from the flow-through cuvette onto a second screen, allowing students to relate the dosing regimen, and the patient's ingestion of a furanocoumarin enzyme inhibitor, to the patient's PK response.

Almost all of the experiments described here used methylene blue to represent drug. With the availability of a suitable quantitative assay method, any drug may be administered to the simulator, thereby enhancing the realism of the students' experience and allowing incorporation of training in analytical procedures to the PK laboratory class.

The ease of construction of this relatively inexpensive apparatus should facilitate introduction of the simulator into laboratory class modules for life science students and for future health care professionals. The versatility of the apparatus also allows instructors to design a practical class to focus on one or more specific aspects of PK theory, according to the needs of their student population. In this regard, construction of a modified apparatus lacking a second compartment (and thus a TISSUE pump), as well as use of varied doses to preclude the need for the ORAL BIOAVAILABILITY pump, would reduce both complexity and cost, while retaining the means to demonstrate those core concepts related to repeated dosing that may be more important for a clinical student population. When the ADAM was introduced into the classroom in our undergraduate pharmacology programme, students reported increased confidence in analysing and interpreting PK data, and these observations were supported by measured improvements in their ability to solve PK graphing and calculation problems successfully. Our observations suggest that the ADAM represents an effective and unique addition to the armoury of those tasked with teaching the principles of PK, one that complements existing didactic and *in silico* approaches and that offers the promise of improved competence in PK in our future health care professionals.

Competing Interests

This work was supported by grants from the Canadian Institutes of Health Research (MOP55729) and from the Teaching and Learning Enhancement Fund, University of Alberta (Res0025997) to A.H. I.Z. received scholarship support from the Canadian Institutes of Health Research, the Faculty of Graduate Studies & Research and the Faculty of Medicine and Dentistry at the University of Alberta.

References

1 Jambhekar SS, Breen PJ. Basic Pharmacokinetics, 2nd edn. Pharmaceutical Press: London, UK, 2012.

2 Schneider J, Munro I, Krishnan S. Flipping the classroom for pharmacokinetics. Am J Educ Res 2014; 2: 1225–9.

3 Swanson PM, Swanson H. A pilot study on the use of lecture tools to enhance the teaching of pharmacokinetics and pharmacodynamics. J Med Educ Curr Dev 2014; 1: 23–8.

4 Feldman RD, Schoenwald R, Kane J. Development of a computer-based instructional system in pharmacokinetics: efficacy in clinical pharmacology teaching for senior medical students. J Clin Pharmacol 1989; 29: 158–61.

5 Brackett CC, Reuning RH. Teaching pharmacokinetics using a student-centered, modified mastery-based approach. Am J Pharm Educ 1999; 63: 272–7.

6 Dupuis RE, Persky AM. Use of case-based learning in a clinical pharmacokinetics course. Am J Pharm Educ 2008; 72: 29.

7 Persky AM, Stegall-Zanation J, Dupuis RE. Students perceptions of the incorporation of games into classroom instruction for basic and clinical pharmacokinetics. Am J Pharm Educ 2007; 71: 21.

8 Persky AM. The impact of team-based learning on a foundational pharmacokinetics course. Am J Pharm Educ 2012; 76: 31.

9 Woodman OL, Dodds AE, Frauman AG, Mosepele M. Teaching pharmacology to medical students in an integrated problem-based learning curriculum: an Australian perspective. Acta Pharmacol Sin 2004; 25: 1195–203.

10 Brocks DR. uSIMPK. An Excel for Windows-based simulation program for instruction of basic pharmacokinetics principles to pharmacy students. Comput Methods Programs Biomed 2015; 120: 154–63.

11 Haffey F, Brady RR, Maxwell S. Smartphone apps to support hospital prescribing and pharmacology education: a review of current provision. Br J Clin Pharmacol 2014; 77: 31–8.

12 McQueen DS, Begg MJ, Maxwell SR. eDrugCalc: an online self-assessment package to enhance medical students' drug dose calculation skills. Br J Clin Pharmacol 2010; 70: 492–9.

13 Lehmann DF. Teaching from catastrophe: using therapeutic misadventures from hydromorphone to teach key principles in clinical pharmacology. J Clin Pharmacol 2011; 51: 1596–602.

14 Gumtow RH, Proudfoot J, Talada A. An *in vitro* pharmacokinetic system for use in the undergraduate pharmaceutics laboratory: a

one- and two-compartment pharmacokinetic bench model; the glassman patient. Am J Pharm Educ 1988; 52: 117–21.

15 Tucker S. Open your Is and you won't fall off the bicycle. Pharmacol Matters 2014; 7: 10–2.

16 Zhang Y, Huo M, Zhou J, Xie S. PKSolver: an add-in program for pharmacokinetic and pharmacodynamic data analysis in Microsoft Excel. Comput Methods Programs Biomed 2010; 99: 306–14.

17 Fan J, de Lannoy IA. Pharmacokinetics. Biochem Pharmacol 2014; 87: 93–120.

18 Riegelman S, Loo J, Rowland M. Concept of a volume of distribution and possible errors in evaluation of this parameter. J Pharm Sci 1968; 57: 128–33.

19 Greenblatt DJ, Abernethy DR, Divoll M. Is volume of distribution at steady state a meaningful kinetic variable? J Clin Pharmacol 1983; 23: 391–400.

20 Mehvar R. The importance of active learning and practice on the students' mastery of pharmacokinetic calculations for the intermittent intravenous infusion dosing of antibiotics. BMC Med Educ 2012; 12: 116.

21 Keijsers CJ, Segers WS, de Wildt DJ, Brouwers JR, Keijsers L, Jansen PA. Implementation of the WHO-6-step method in the medical curriculum to improve pharmacology knowledge and pharmacotherapy skills. Br J Clin Pharmacol 2015; 79: 896–906.

22 Lesar TS, Briceland L, Stein DS. Factors related to errors in medication prescribing. JAMA 1997; 277: 312–7.

23 Dean B, Schachter M, Vincent C, Barber N. Causes of prescribing errors in hospital inpatients: a prospective study. Lancet 2002; 359: 1373–8.

24 Boreham NC, Mawer GE, Foster RW. Medical students' errors in pharmacotherapeutics. Med Educ 2000; 34: 188–93.

25 Keijsers CJ, Brouwers JR, de Wildt DJ, Custers EJ, Ten Cate OT, Hazen AC, *et al*. A comparison of medical and pharmacy students' knowledge and skills of pharmacology and pharmacotherapy. Br J Clin Pharmacol 2014; 78: 781–8.